References

1 Makol A, Watt KD, Chowdhary VR. Autoimmune hepatitis: a review of current diagnosis and treatment. Hepat Res Treat 2011; **2011**:390916.

2 Oo YH, Hubscher SG, Adams DH. Autoimmune hepatitis: new paradigms in the pathogenesis, diagnosis, and management. Hepatol Int 2010; **4**:475–93.

3 Longhi MS, Ma Y, Mieli-Vergani G, Vergani D. Adaptive immunity in autoimmune hepatitis. Dig Dis 2010; **28**:63–9.

4 Dienes HP, Drebber U. Pathology of immune-mediated liver injury. Dig Dis 2010; **28**:57–62.

5 Ichiki Y, Aoki CA, Bowlus CL, Shimoda S, Ishibashi H, Gershwin ME. T cell immunity in autoimmune hepatitis. Autoimmun Rev 2005; **4**:315–21.

6 Suzuki Y, Kobayashi M, Hosaka T *et al.* Peripheral $CD8^+/CD25^+$ lymphocytes may be implicated in hepatocellular injuries in patients with acute-onset autoimmune hepatitis. J Gastroenterol 2004; **39**:649–53.

7 Fox CK, Furtwaengler A, Nepomuceno RR, Martinez OM, Krams SM. Apoptotic pathways in primary biliary cirrhosis and autoimmune hepatitis. Liver 2001; **21**:272–9.

8 Senaldi G, Portmann B, Mowat AP, Mieli-Vergani G, Vergani D. Immunohistochemical features of the portal tract mononuclear cell infiltrate in chronic aggressive hepatitis. Arch Dis Child 1992; **67**:1447–53.

9 MacDonald HR. Development and selection of NKT cells. Curr Opin Immunol 2002; **14**:250–4.

10 Morita M, Motoki K, Akimoto K *et al.* Structure–activity relationship of alpha-galactosylceramides against B16-bearing mice. J Med Chem 1995; **38**:2176–87.

11 Kawano T, Cui J, Koezuka Y *et al.* CD1d-restricted and TCR-mediated activation of valpha14 NKT cells by glycosylceramides. Science 1997; **278**:1626–9.

12 Bendelac A, Savage PB, Teyton L. The biology of NKT cells. Annu Rev Immunol 2007; **25**:297–336.

13 Jahng AW, Maricic I, Pedersen B *et al.* Activation of natural killer T cells potentiates or prevents experimental autoimmune encephalomyelitis. J Exp Med 2001; **194**:1789–99.

14 Singh AK, Wilson MT, Hong S *et al.* Natural killer T cell activation protects mice against experimental autoimmune encephalomyelitis. J Exp Med 2001; **194**:1801–11.

15 Furlan R, Bergami A, Cantarella D *et al.* Activation of invariant NKT cells by alphaGalCer administration protects mice from MOG35-55-induced EAE: critical roles for administration route and IFN-gamma. Eur J Immunol 2003; **33**:1830–8.

16 Hong S, Wilson MT, Serizawa I *et al.* The natural killer T-cell ligand alpha-galactosylceramide prevents autoimmune diabetes in non-obese diabetic mice. Nat Med 2001; **7**:1052–6.

17 Naumov YN, Bahjat KS, Gausling R *et al.* Activation of CD1d-restricted T cells protects NOD mice from developing diabetes by regulating dendritic cells subsets. Proc Natl Acad Sci USA 2001; **98**:13838–43.

18 Wang B, Geng YB, Wang CR. CD1-restricted NKT cells protect nonobese diabetic mice from developing diabetes. J Exp Med 2001; **194**:313–20.

19 Matsuda JL, Naidenko OV, Gapin L *et al.* Tracking the response of natural killer T cells to a glycolipid antigen using CD1d tetramers. J Exp Med 2000; **192**:741–54.

20 Geissmann F, Cameron TO, Sidobre S *et al.* Intravascular immune surveillance by $CXCR6^+$ NKT cells patrolling liver sinusoids. PLoS Biol 2005; **3**:e113.

21 Exley MA, Koziel MJ. To be or not to be NKT : natural killer T cells in the liver. Hepatology 2004; **40**:1033–40.

22 Takeda K, Hayakawa Y, Van Kaer L, Matsuda H, Yagita H, Okumura K. Critical contribution of liver natural killer T cells to murine model of hepatitis. Proc Natl Acad Sci USA 2000; **97**:5498–503.

23 Swain MG. Hepatic NKT cells: friend or foe? Clin Sci (Lond) 2008; **114**:457–66.

24 Tamaki S, Homma S, Enomoto Y *et al.* Autoimmune hepatic inflammation by vaccination of mice with dendritic cells loaded with well-differentiated hepatocellular carcinoma cells and administration of interleukin-12. Clin Immunol 2005; **117**:280–93.

25 Saeki C, Nakano M, Takahashi H *et al.* Accumulation of functional regulatory T cells in actively inflamed liver in mouse dendritic cell-based autoimmune hepatic inflammation. Clin Immunol 2010; **135**:156–66.

26 Trinchieri G. Interleukin-12 and the regulation of innate resistance and adaptive immunity. Nat Rev Immunol 2003; **3**:133–46.

27 Biburger M, Tiegs G. Alpha-galactosylceramide-induced liver injury in mice is mediated by TNF-alpha but independent of Kupffer cells. J Immunol 2005; **175**:1540–50.

28 Eksteen B, Afford SC, Wigmore SJ, Holt AP, Adams DH. Immune-mediated liver injury. Semin Liver Dis 2007; **27**:351–66.

29 Vergani D, Choudhuri K, Bogdanos DP, Mieli-Vergani G. Pathogenesis of autoimmune hepatitis. Clin Liver Dis 2002; **6**:727–37.

30 Kaneko Y, Harada M, Kawano T *et al.* Augmentation of Valpha14 NKT cell-mediated cytotoxicity by interleukin 4 in an autocrine mechanism resulting in the development of concanavalin A-induced hepatitis. J Exp Med 2000; **191**:105–14.

31 Sprengers D, Sillé FC, Derkow K *et al.* Critical role for CD1d-restricted invariant NKT cells in stimulating intrahepatic CD8 T-cell responses to liver antigen. Gastroenterology 2008; **134**:2132–43.

32 Mattner J, Savage PB, Leung P *et al.* Liver autoimmunity triggered by microbial activation of natural killer T cells. Cell Host Microbe 2008; **3**:304–15.

33 Kinjo Y, Wu D, Kim G *et al.* Recognition of bacterial glycosphingolipids by natural killer T cells. Nature 2005; **434**:520–5.

34 Mattner J, Debord KL, Ismail N *et al.* Exogenous and endogenous glycolipid antigens activate NKT cells during microbial infections. Nature 2005; **434**:525–9.

35 Porubsky S, Speak AO, Luckow B, Cerundolo V, Platt FM, Gröne HJ. Normal development and function of invariant natural killer T cells in mice with isoglobotrihexosylceramide (iGb3) deficiency. Proc Natl Acad Sci USA 2007; **104**:5977–82.

36 Ehlers M, Ravetch JV. Opposing effects of Toll-like receptor stimulation induce autoimmunity or tolerance. Trends Immunol 2007; **28**:74–9.

37 Marshak-Rothstein A. Toll-like receptors in systemic autoimmune disease. Nat Rev Immunol 2006; **6**:823–35.

Supporting information

Additional supporting information may be found in the online version of this article.

Fig. S1. The dynamic statistics of natural killer (NK) T cells in the autoimmune hepatic inflammation (AHI) liver and spleen. (A) Absolute number of NK T cells in the liver (a) and spleen (b) in AHI. The number was determined as [total number of mononuclear cells (MNCs) in the liver or spleen] × [the frequency of $CD3^+NK1{\cdot}1^+$ cells] in each group [$n = 5$, mean ± standard deviation (s.d.), $^*P < 0{\cdot}001$]. (B) (a) Population of intrahepatic $CXCR6^+$ NK T cells ($n = 5$, mean ± s.d., $^*P < 0{\cdot}001$). (b) Expression of CXCL16 in hepatic tissue. Levels of CXCL16 mRNA in each group were determined by quantitative reverse transcription–polymerase chain reaction (qRT–PCR). Bars indicate mean ± s.d., $^*P < 0{\cdot}001$. (C) (a) Frequency of interferon (IFN)-γ^+ NK T cells in each group ($n = 5$, mean ± s.d., $^*P < 0{\cdot}001$). (b) Frequency of interleukin (IL)-4^+ NK T cells in each group. All experiments were repeated at least three times.

Fig. S2. Frequency of natural killer (NK) T cells in the liver and spleen in autoimmune hepatic inflammation (AHI). Frequencies of NK T cells in intrahepatic major histocompatibility complexes (MHCs) and splenocytes were determined by flow cytometry ($n = 5$, mean ± standard deviation, $^*P < 0{\cdot}001$). Experiments were repeated at least three times.

World Journal of Gastroenterology

Online Submissions: http://www.wjgnet.com/esps/
wjg@wjgnet.com
doi:10.3748/wjg.v18.i31.4118

World J Gastroenterol 2012 August 21; 18(31): 4118-4126
ISSN 1007-9327 (print) ISSN 2219-2840 (online)

ORIGINAL ARTICLE

Efficacy of MK615 for the treatment of patients with liver disorders

Atsushi Hokari, Tomohisa Ishikawa, Hisao Tajiri, Takahide Matsuda, Osamu Ishii, Nobuyuki Matsumoto, Chiaki Okuse, Hideaki Takahashi, Takeshi Kurihara, Ko-ichi Kawahara, Ikuro Maruyama, Mikio Zeniya

Atsushi Hokari, Tomohisa Ishikawa, Hisao Tajiri, Mikio Zeniya, Department of Internal Medicine, Division of Gastroenterology and Hepatology, The Jikei University School of Medicine, Tokyo 1058471, Japan
Takahide Matsuda, Osamu Ishii, Department of Internal Medicine, Division of General Internal Medicine, St. Marianna University School of Medicine, Kawasaki 2168511, Japan
Nobuyuki Matsumoto, Chiaki Okuse, Hideaki Takahashi, Department of Internal Medicine, Division of Gastroenterology and Hepatology, St. Marianna University School of Medicine, Kawasaki 2168511, Japan
Takeshi Kurihara, Keio University, Graduate School of Media and Governance, Fujisawa 2520882, Japan
Ko-ichi Kawahara, Department of Biomedical Engineering, Osaka Institute of Technology, Osaka 5358585, Japan
Ikuro Maruyama, Department of Systems Biology in Thromboregulation, Kagoshima University Graduate School of Medical and Dental Sciences, Kagoshima 8908580, Japan
Author contributions: Kawahara K, Maruyama I, Zeniya M designed the research; Hokari A, Ishikawa T, Tajiri H, Matsuda T, Ishii O, Matsumoto N, Okuse C, Takahashi H, Kurihara T, Zeniya M performed the research; Hokari A, Zeniya M analyzed the data; and Hokari A and Zeniya M wrote the paper.
Correspondence to: Dr. Mikio Zeniya, Department of Internal Medicine, Division of Gastroenterology and Hepatology, The Jikei University School of Medicine, Nishi-shimbashi 3-25-8, Minato-ku, Tokyo 1058471, Japan. zeniya@jikei.ac.jp
Telephone: +81-3-34331111 Fax: +81-3-34350569
Received: December 8, 2011 Revised: May 10, 2012
Accepted: May 26, 2012
Published online: August 21, 2012

Abstract

AIM: To investigate the hepatoprotective effect of MK615, a Japanese apricot extract, in an animal model, and its clinical therapeutic effect.

METHODS: Wistar rats were administered physiological saline (4 mL/kg) or MK615 solution (4 mL/kg) for 7 d. On the sixth d, acute hepatic injury was induced by administering a single intraperitoneal injection (*ip*) of D-galactosamine hydrochloride (D-GalN) (600 mg/kg). Plasma levels of alanine aminotransferase (ALT) and aspartate aminotransferase (AST) were determined, and liver tissues were used for histopathological analysis. Fifty-eight patients with liver disorders [hepatitis C (n = 40), non-alcoholic fatty liver disease (n = 15), and autoimmune liver disease (n = 3)] were orally administered commercially available Misatol ME-containing MK615 (13 g/d) daily for 12 wk. Blood and urine were sampled immediately before and 6 wk, 12 wk, and 16 wk after the start of intake to measure various biochemical parameters. The percentage change in ALT and AST levels after 12 wk from the pre-intake baseline served as a primary endpoint.

RESULTS: D-GalN effectively induced acute hepatic injury in the rats. At 48 h after the *ip* injection of D-GalN, the plasma levels of ALT (475.6 ± 191.5 IU/L *vs* 225.3 ± 194.2 IU/L, $P < 0.05$) and AST (1253.9 ± 223.4 IU/L *vs* 621.9 ± 478.2 IU/L, $P < 0.05$) in the MK615 group were significantly lower than the control group. Scattered single cell necrosis, loss of hepatocytes, and extensive inflammatory cell infiltration were observed in hepatic tissue samples collected from the control group. However, these findings were less pronounced in the group receiving MK615. At the end of the clinical study, serum ALT and AST levels were significantly decreased compared with pre-intake baseline levels from 103.5 ± 58.8 IU/L to 71.8 ± 39.3 IU/L ($P < 0.05$) and from 93.5 ± 55.6 IU/L to 65.5 ± 34.8 IU/L ($P < 0.05$), respectively. A reduction of ⩾ 30% from the pre-study baseline ALT level was observed in 26 (45%) of the 58 patients, while 25 (43%) patients exhibited similar AST level reductions. The chronic hepatitis C group exhibited significant ALT and AST level reductions from 93.4 ± 51.1 IU/L to 64.6 ± 35.1 IU/L ($P < 0.05$) and from 94.2 ± 55.5 IU/L to 67.2 ± 35.6 IU/L ($P < 0.05$), respectively. A reduction of ⩾ 30% from the pre-study baseline ALT level was observed in 20 (50%) of the 40 patients.

ALT levels in both the combined ursodeoxycholic acid (UDCA) treatment and the UDCA uncombined groups were significantly lower after Misatol ME administration. MK615 protected hepatocytes from D-GalN-induced cytotoxicity in rats. Misatol ME decreased elevated ALT and AST levels in patients with liver disorders.

CONCLUSION: These results suggest that MK615 and Misatol ME are promising hepatoprotective agents for patients with liver disorders.

Key words: *Prunus mume*; MK615; Liver damage; Hepatitis C; Non-alcoholic fatty liver disease

Peer reviewer: Marek Hartleb, Department of Gastroenterology and Hepatology, Medical University of Silesia, 70-111 Szczecin, Poland

Hokari A, Ishikawa T, Tajiri H, Matsuda T, Ishii O, Matsumoto N, Okuse C, Takahashi H, Kurihara T, Kawahara K, Maruyama I, Zeniya M. Efficacy of MK615 for the treatment of patients with liver disorders. *World J Gastroenterol* 2012; 18(31): 4118-4126 Available from: URL: http://www.wjgnet.com/1007-9327/full/v18/i31/4118.htm DOI: http://dx.doi.org/10.3748/wjg.v18.i31.4118

INTRODUCTION

Japanese apricot (*Prunus mume* Sieb. et Zucc.), hereinafter referred to as *ume*, was brought to Japan from China around the eighth century. The flesh of this fruit has been used not only as food but also as medicine. *Ishinho*, the oldest medical monograph in Japan, which was written in AD 984, indicates that both *umeboshi* (pickled *ume*) and *ubai* (smoke-dried *ume*) were used as medicines (e.g., as anti-diarrheal agents and for detoxification in food or drug poisoning). *Shokokukodenhiho*, published in 1817, also refers to the effectiveness of *ume* extracts. It is thus evident that *ume* was used extensively as a folk remedy in Japan. Syringaresinol, a lignan in *ume*, was recently shown to control infection by inhibiting the migration of *Helicobacter pylori*[1]. MK615, an extract from Japanese apricot, contains triterpenoids such as ursolic acid (UA)[2], oleanolic acid (OA)[2-4], lupeol[2,4], α-amyrin[2], and β-sitosterol[4]. These substances have been shown to exert various biological actions. Reports have described diverse effects, including anti-tumor activity (against tumor cell lines such as those of gastric cancer[5], leukemia[5], breast cancer[4,6], hepatocellular carcinoma[7,8], colon cancer[9], pancreatic cancer[10], and malignant melanoma[11]) and immunopotentiation in experimental animals exposed to X-rays[4]. MK615 was previously reported to inhibit the release of high-mobility group box 1 (HMGB1) from lipopolysaccharide (LPS)-stimulated macrophage-like RAW264.7 cells and to activate the transcription factor nuclear factor erythroid 2-related factor 2 (Nrf2), resulting in the induction of heme oxygenase-1 (HO-1). MK615 was also shown to suppress the formation of inflammation-inducing cytokines [tumor necrosis factor α (TNF-α) and interleukin-6 (IL-6)] by inactivating mitogen-activated protein kinases (MAPKs) and the transcription factor nuclear factor-κB (NF-κB)[3,12]. It is thus evident that *ume* extracts exert anti-inflammatory and antioxidative actions. However, the significance of these actions in the liver has not been adequately clarified.

Given the anti-inflammatory and antioxidative actions of MK615, we investigated the hepatoprotective effects of MK615. In addition, the effects of Misatol ME, a beverage containing MK615 that is approved as a health food product in Japan, were clinically evaluated in patients with liver disorders that included hepatitis C, chronic inflammation of the liver, as well as fatty liver disease, which is closely involved in oxidative stress.

MATERIALS AND METHODS

Effect of MK615 on D-galactosamine hydrochloride-induced acute hepatic injury in rats

Preparation of MK615 solution: MK615 solution was prepared from a condensed extract of *ume*. In brief, *ume* were squeezed using a press, and the *ume* juice was then heated and concentrated 20-fold[5]. The condensed extract was neutralized using NaOH and was then heat-sterilized. The MK615 solution contained the neutral, condensed *ume* extract.

D-galactosamine hydrochloride-induced hepatic injury in rats: Seven-week-old male Wistar rats (Crlj:WI) weighing 200-240 g were purchased from Charles River Laboratories Japan (Yokohama, Japan). All rats were maintained under controlled temperature and lighting conditions (12/12-h dark/light cycle), and water and standard diet were provided ad libitum in accordance with the institute's guidelines for care and use of laboratory animals in research.

Acute hepatic injury was induced by administering a single intraperitoneal (*ip*) injection of D-galactosamine hydrochloride (D-GalN) (600 mg/kg; Wako Pure Chemical Industries, Osaka, Japan). In this study, rats were divided into 3 experimental groups. In group I (the vehicle control group), rats were administered physiological saline (4 mL/kg per day) *via* gavage for 7 d and injected with D-GalN (*ip*) 2 h after the sixth oral administration of saline (6 d from the first oral administration). In group II (the MK615 group), rats received MK615 solution (4 mL/kg per day) *via* gavage for 7 d and were injected with D-GalN (*ip*) 2 h after the sixth oral administration of MK615 solution. In group III, rats were administered the neutral MK615 solution (4 mL/kg per day) *via* gavage for 7 d and were injected with saline (*ip*) 2 h after the sixth oral administration of MK615 solution. group III served as a negative experimental control without D-GalN-induced hepatic injury (Figure 1). Treatments involving oral administration by gavage were conducted between

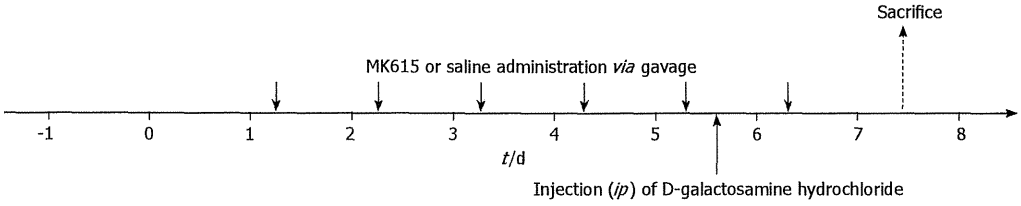

Figure 1 Experiment protocol of D-galactosamine hydrochloride-induced acute hepatic injury in rats.

9:00 and 10:00 AM and *ip* injections were administered between 11:00 AM and 12:00 noon. All rats were sacrificed by exsanguination under anesthesia 48 h after the *ip* injection of D-GalN or saline (8 d after the first oral administration). Blood samples from the abdominal aorta were immediately heparinized, and plasma samples were isolated by centrifugation. Plasma samples were frozen and stored at -80 ℃ until used, and subsequently analyzed to determine the levels of alanine aminotransferase (ALT) and aspartate aminotransferase (AST). Liver tissue samples were also obtained from each rat and used for histopathological analysis. The plasma levels of ALT and AST were determined using a commercially available analytical kit (Transaminase CII-Test; Wako Pure Chemical Industries).

Evaluation of the effects of MK615 in patients with liver disorder

Subjects: This study involved patients who were definitively diagnosed with a liver disorder at the Jikei University School of Medicine Hospital, the St. Marianna University School of Medicine Hospital, or the Kurihara Clinic between December 2007 and December 2009 and who met the following requirements: (1) ALT level exceeding reference limits when tested within 3 mo before the start of this study, indicating the presence of hepatopathy; (2) serum hepatitis C virus (HCV)-RNA positivity (determined by real-time polymerase chain reaction) in patients with chronic hepatitis C; and (3) presence of fatty liver confirmed by diagnostic imaging in cases of non-alcoholic fatty liver disease (NAFLD). The following patients were excluded from the study: (1) those receiving treatment for liver cirrhosis, hepatocellular carcinoma, or other malignant tumors; (2) patients receiving treatment with Stronger Neo-Minophagen C; (3) those receiving treatment with interferon (IFN); and (4) habitual drinkers (alcohol consumption, > 30 g/d) or occasional heavy drinkers. Concomitant use of drugs or any treatment with antiviral, immunomodulating, or marrow-suppressive activity was prohibited during the study period, but continued use of drugs that had been initiated before the study was permitted. No patients were heavy drinkers. The ethics committee of each participating facility approved the study protocol. Informed consent to participate in the study was obtained in writing from all patients.

Methods: In Japan, MK615 solution is commercially available as Misatol ME (AdaBio Co. Ltd., Takasaki, Japan). For the clinical study, Misatol ME was used as the MK615 solution and was ingested orally every d (2 × 6.5 g packs/d) for 12 wk. Blood and urine were sampled immediately before and 6 wk, 12 wk, and 16 wk after the start of MK615 intake to measure the following parameters: white blood cell (WBC) count, differential leukocyte count, red blood cell (RBC) count, hemoglobin, hematocrit, platelet count, ALT, AST, γ-glutamyl transpeptidase (γ-GTP), alkaline phosphatase (ALP), total protein, albumin, total cholesterol, cholinesterase, and total bilirubin, as well as urinalysis parameters. The percentage change in ALT and AST levels after 12 wk of intake from the pre-intake baseline served as primary and secondary endpoints, respectively. In the analysis of these endpoints, an improvement of ≥ 50% from the pre-intake baseline was regarded "markedly effective", ≥ 30% was regarded "effective", ≤ 30% as "ineffective", and an aggravation of ≥ 30% as "worsened". The response rate was defined as the percentage of "markedly effective" plus "effective" cases.

Statistical analysis

Data are expressed as mean ± SD. Statistical analyses were performed using Stat View for Windows Version 5.0 (SAS Institute Inc., North Carolina, United States). Differences between 2 groups were analyzed using the Mann-Whitney *U* test. Comparisons between baseline and each time point were performed using Dunnett's test. $P < 0.05$ was considered significant.

RESULTS

The effect of MK615 on D-galactosamine hydrochloride-induced acute hepatic injury in rats

ALT and AST plasma levels in control rats were elevated 48 h after D-GalN induction, with mean values of 475.6 ± 191.5 IU/L ($n = 8$) and 1253.9 ± 223.4 IU/L ($n = 8$), respectively. In the MK615 group, the ALT and AST levels were 225.3 ± 194.2 IU/L ($n = 9$) and 621.9 ± 478.2 IU/L ($n = 9$), respectively. The levels of ALT and AST in the MK615 group rats were significantly lower than in those of the control group ($P = 0.0433$ for ALT, $P = 0.0124$ for AST by Mann-Whitney *U* test) (Figure 2A and B).

Liver tissues were obtained from both control group rats and MK615 group rats at 48 h after D-GalN injection. Scattered single cell necrosis (swollen eosinophilic hepatocytes) and loss of hepatocytes was observed in hepatic tissue samples from the control group. Extensive inflammatory cell infiltration was also noted (Figure 2C). Figure 2D shows that these features of D-GalN-induced

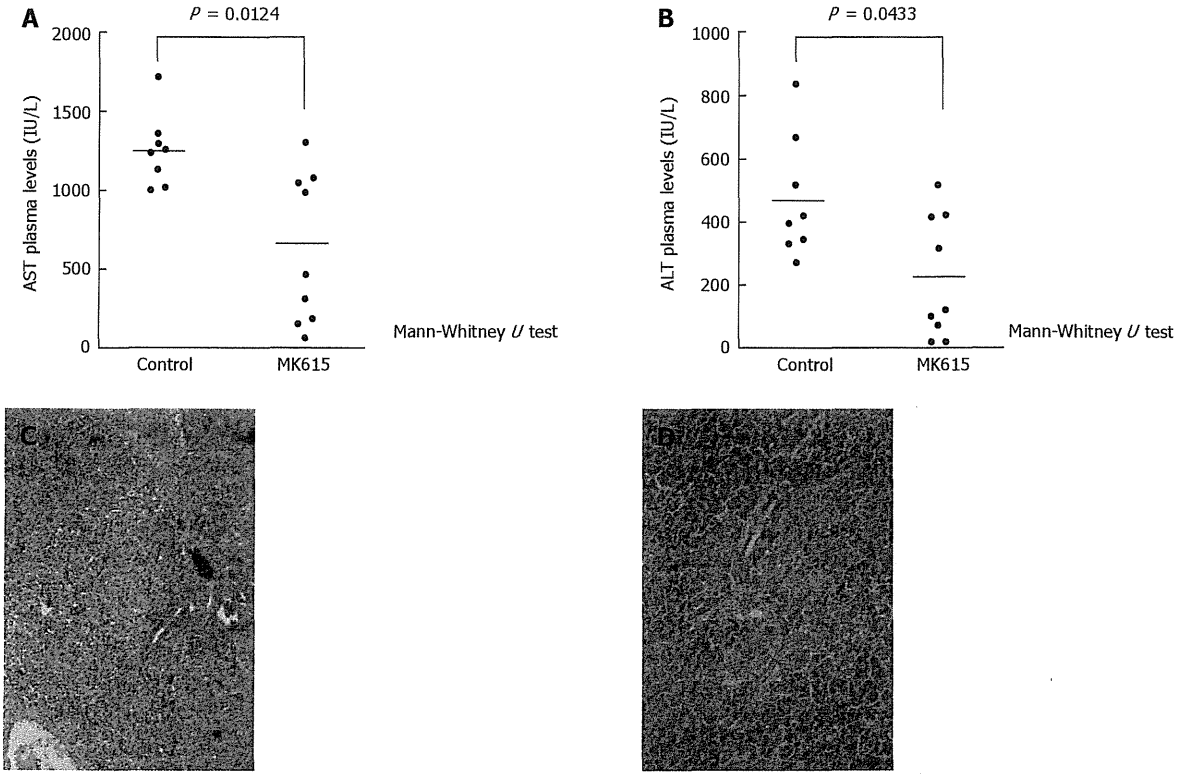

Figure 2 Effect of MK615 in D-galactosamine hydrochloride-induced acute hepatic injury in rats. A: AST plasma levels; B: ALT plasma levels; C: Control group (liver); D: MK615 group (liver). AST:Aspartate aminotransferase; ALT: Alanine aminotransferase.

Table 1 Background of patients with liver disorders

	Chronic hepatitis C	NAFLD	Autoimmune liver disease
Number	40	15	3
Gender (M/F)	25/15	14/1	1/2
Age (yr)	64.4 ± 11.3	52.5 ± 13.7	65.7 ± 4.0
HCV viral load(10^n/mL)	6.2 ± 0.8		
≥ 5log/< 5log/ND	35/3/2		
WBC count (/μL)	4153 ± 994	6800 ± 1578	3967 ± 723
RBC count (10^4/μL)	415 ± 59	490 ± 51	448 ± 48
Hemoglobin (g/dL)	13.1 ± 1.8	15.5 ± 1.1	12.5 ± 1.7
Platelet count (10^4/μL)	13.8 ± 5.7	20.3 ± 8.4	17.2 ± 5.1
AST (IU/L)	94.2 ± 55.5	84.5 ± 50.0	129.3 ± 90.5
ALT (IU/L)	93.4 ± 51.1	131.9 ± 72.5	96.7 ± 50.1
γ-GTP (IU/L)	72.9 ± 60.5	181.9 ± 197.5	120.3 ± 74.2
LDH (IU/L)	237.8 ± 54.8	228.9 ± 44.4	270 ± 44.3
ALP (IU/L)	318.1 ± 116.8	303.4 ± 106.8	391 ± 293.1
Total bilirubin (mg/dL)	0.84 ± 0.29	0.8 ± 0.44	0.67 ± 0.15
Total cholesterol (mg/dL)	162 ± 35.2	188.5 ± 49.1	174.7 ± 40.1
Total protein (g/dL)	7.5 ± 0.6	7.7 ± 0.3	7.9 ± 0.9
Albumin (g/dL)	3.9 ± 0.4	4.4 ± 0.3	3.9 ± 0.9
BUN (mg/dL)	16.2 ± 4.0	13.6 ± 3.2	15.3 ± 3.1
Creatinine (mg/dL)	0.76 ± 0.16	0.75 ± 0.1	0.62 ± 0.06

Data are expressed as the mean ± standard deviation. NAFLD: Non-alcoholic fatty liver disease; ND: Not done; M: Male; F: Female; HCV: Hepatitis C virus; WBC: White blood cell; RBC: Red blood cell; AST: Aspartate aminotransferase; ALT: Alanine aminotransferase; γ-GTP: γ guanosine triphosphate; LDH: Lactate dehydrogenase; ALP: Alkaline phosphatase; BUN: Blood urea nitrogen.

hepatic injury were reduced in the treatment group receiving the MK615 solution.

The effects of MK615 in patients with liver disorders

We enrolled 58 patients in this clinical study (mean age, 61.4 ± 12.7 years; range: 29-82 years; 40 men and 18 women). The diagnosis was chronic hepatitis C in 40 patients, NAFLD in 15 patients, and autoimmune liver disease in 3 patients (2 with autoimmune hepatitis and 1 with primary sclerosing cholangitis). Table 1 lists the background variables in relation to the diseases diagnosed.

Analysis of the entire study population determined that ALT levels had decreased significantly from 103.5 ± 58.8 IU/L before the start of the study to 81.3 ± 45.7 IU/L ($P < 0.05$) at 6 wk, 71.8 ± 39.3 IU/L ($P < 0.05$) at 12 wk, and 72.3 ± 40.3 IU/L ($P < 0.05$) at 16 wk (Figure 3A). AST levels decreased significantly from 93.5 ± 55.6 IU/L before the start of the study to 77.6 ± 47.1 IU/L ($P < 0.05$) at 6 wk, 65.5 ± 34.8 IU/L ($P < 0.05$) at 12 wk, and 68.3 ± 37.8 IU/L ($P < 0.05$) at 16 wk (Figure 3B). A reduction of ≥ 30% from pre-study baseline ALT levels was observed in 26 (45%) of the 58 patients, whereas 25 (43%) patients exhibited a similar reduction in AST levels (Table 2).

When the effects of Misatol ME were analyzed in relation to the disease diagnosed, the chronic hepatitis C group exhibited significant ALT level reductions from the pre-study baseline of 93.4 ± 51.1 IU/L to 75.3 ± 46.6 IU/L ($P < 0.05$) at 6 wk, 64.6 ± 35.1 IU/L ($P < 0.05$) at 12 wk, and 64.6 ± 33.8 IU/L ($P < 0.05$) at 16 wk (Figure

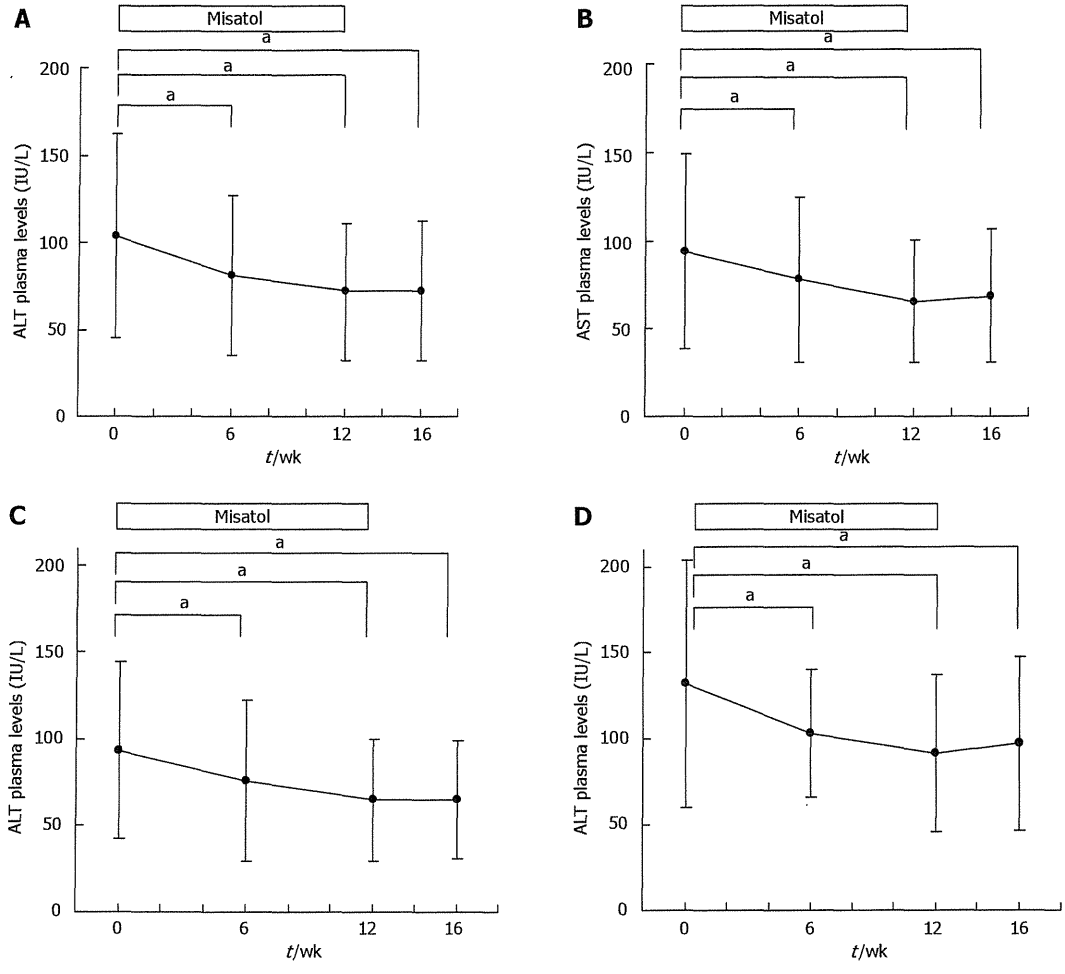

Figure 3 Effects of MK615 in patients with liver disorder, chronic hepatitis C and non-alcoholic fatty liver disease. A: Alanine aminotransferase (ALT); B: Aspartate aminotransferase (AST); C: Chronic hepatitis C group (ALT); D: Non-alcoholic fatty liver disease group (ALT). $^{a}P < 0.05$ *vs* 0 wk group. Dunnett's test.

Table 2 Response rate of MK615 therapy in patients with liver disorder (%)

	ALT	AST
Chronic hepatitis C	20/40 (50)	16/40 (40)
NAFLD	5/15 (33)	6/15 (40)
Autoimmune liver disease	1/3 (33)	3/3 (100)
Total	26/58 (45)	25/58 (43)

NAFLD: Non-alcoholic fatty liver disease; AST: Aspartate aminotransferase; ALT: Alanine aminotransferase.

3C). This same group of patients exhibited significant AST level reductions from the pre-study baseline of 94.2 ± 55.5 IU/L to 78.8 ± 49.5 IU/L ($P < 0.05$) at 6 wk, 67.2 ± 35.6 IU/L ($P < 0.05$) at 12 wk, and 66.6 ± 33.7 IU/L ($P < 0.05$) at 16 wk. In the chronic hepatitis C group, a reduction of ≥ 30% from the pre-study baseline ALT level was observed in 20 (50%) of the 40 patients, while 16 (40%) patients exhibited similar AST level reductions (Table 2). Among the patients with chronic hepatitis C, ALT data before the start of test beverage intake (24 wk before starting intake) were available for 32 patients. These patients were subdivided into combined ursodeoxycholic acid (UDCA) treatment ($n = 20$) (Figure 4A) and UDCA uncombined ($n = 12$) groups (Figure 4B). In both the combined UDCA treatment and UDCA uncombined groups, ALT levels were significantly lower after the intake of Misatol ME compared with those before intake.

The NAFLD group exhibited significant ALT level reductions from 131.9 ± 72.5 IU/L before the start of the study to 102.8 ± 37.6 IU/L ($P < 0.05$) at 6 wk, 90.9 ± 45.6 IU/L ($P < 0.05$) at 12 wk, and 96.9 ± 50.8 IU/L ($P < 0.05$) at 16 wk (Figure 3D). This group also exhibited significant AST level reductions during the Misatol ME intake period compared with the pre-start baseline level; levels were 84.5 ± 50.0 IU/L before the start of the study, 66.7 ± 24.2 IU/L ($P < 0.05$) at 6 wk, 58.1 ± 26.0 IU/L ($P < 0.05$) at 12 wk, and 69.8 ± 41.9 IU/L (NS) at 16 wk. In the NAFLD group, a reduction of ≥ 30% from the pre-study baseline ALT level was observed in 5 (33%) of the 15 patients, whereas similar AST level reductions were observed in 6 (40%) patients (Table 2).

The levels of γ-GTP in the entire study population also decreased significantly after Misatol ME intake compared with pre-intake baseline levels (data not shown).

Table 3 presents the hematological and biochemical

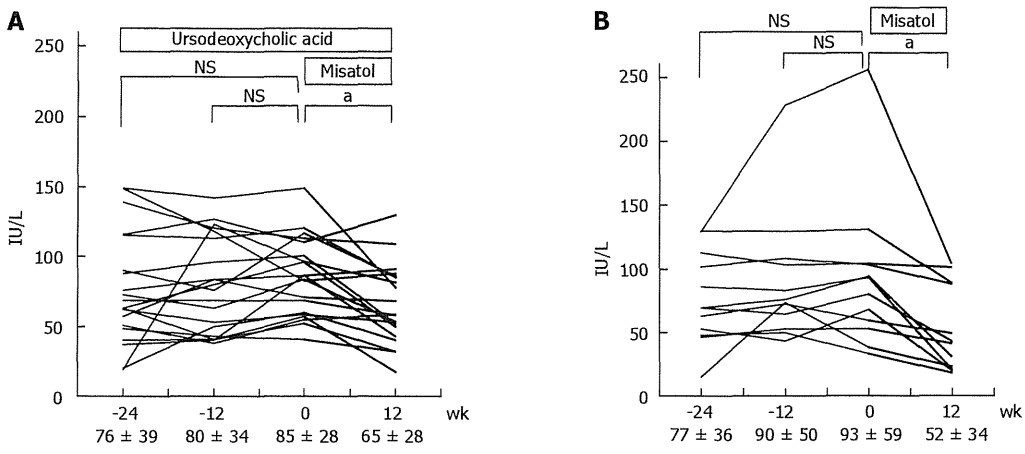

Figure 4 Effects of MK615 in patients with chronic hepatitis C (alanine aminotransferase). A: Misatol was added on ursodeoxycholic acid; B: Only Misatol was used. [a]$P < 0.05$ *vs* 0 wk group. Dunnett's test. NS: Not significant.

Table 3 Changes of serum level during MK615 therapy in patients with liver disorders

	Before therapy	During therapy 12 wk	*P* value[1]
WBC count (/μL)	4828 ± 1640	4977 ± 1855	NS
RBC count (10^4/μL)	436 ± 65	435 ± 65	NS
Hemoglobin (g/dL)	13.7 ± 2.0	13.8 ± 1.9	NS
Platelet count (10^4/μL)	15.7 ± 7.0	15.6 ± 6.6	NS
AST (IU/L)	94 ± 56	66 ± 35	< 0.05
ALT (IU/L)	104 ± 59	72 ± 39	< 0.05
γ-GTP (IU/L)	104 ± 121	74 ± 93	< 0.05
LDH (IU/L)	237 ± 52	227 ± 52	< 0.05
ALP (IU/L)	318 ± 124	298 ± 126	< 0.05
Total bilirubin (mg/dL)	0.8 ± 0.3	0.8 ± 0.3	NS
Total cholesterol (mg/dL)	170 ± 40	171 ± 43	NS
Total protein (g/dL)	7.6 ± 0.6	7.6 ± 0.5	NS
Albumin (g/dL)	4.0 ± 0.5	4.1 ± 0.4	NS
BUN (mg/dL)	15.5 ± 3.9	14.7 ± 3.5	NS
Creatinine (mg/dL)	0.75 ± 0.15	0.74 ± 0.15	NS

Data are expressed as the mean ± standard deviation. [1]Dunnett's test. NS: Not significant; WBC: White blood cell; RBC: Red blood cell; AST: Aspartate aminotransferase; ALT: Alanine aminotransferase; γ-GTP: γ-guanosine triphosphate; LDH: Lactate dehydrogenase; ALP: Alkaline phosphatase; BUN: Blood urea nitrogen; NS: Not significant.

data obtained for the clinical study. No change associated with Misatol ME intake was noted in any hematological or biochemical parameter other than in the indicators of liver function, which improved after MK615 intake. An unexplained eruption was observed in 1 patient with NAFLD, which was the only adverse event observed during this study, and was not found to have a causal relationship with the intake of Misatol ME.

DISCUSSION

This is the first study demonstrating that Misatol ME (a beverage containing MK615, an *ume* extract) lowers blood transaminase levels in patients with liver disorders such as chronic hepatitis C and NAFLD. *ume* has been used as traditional medicine and food in Japan since ancient times[5]. The clinical effects of *ume* have been attributed to the biological activity of MK615. MK615 contains triterpenoids such as OA, UA, lupeol, α-amyrin, and β-sitosterol[2-4], and has been shown to exert anti-tumor activity against various tumor cell lines, including those of gastric cancer[5], leukemia[5], breast cancer[4,6], hepatocellular carcinoma[7,8], colorectal cancer[9], pancreatic cancer[10], esophageal cancer[2], and malignant melanoma[11]. The possible mechanisms underlying the anti-tumor activity of MK615 include induction of apoptosis[2,6,9,11], induction of autophagy[9], cell cycle arrest[2,6,7,10], reduced expression of receptors for advanced glycation end products (RAGE) on membrane surfaces of cancer cells[8,11], and immunopotentiation following exposure to X-rays[4]. MK615 inhibits the release of HMGB1 from mouse macrophage-like RAW264.7 cells[3]. This inhibitory activity is mediated by Nrf2 activation and HO-1 induction, suggesting that MK615 possesses antioxidative activity[3]. The authors also previously demonstrated that MK615 suppressed the release of the inflammatory cytokines TNF-α and IL-6 in RAW264.7 cells[12]. This suppression was mediated by the inactivation of MAPKs and NF-κB, thus indicating an anti-inflammatory effect of MK615[12].

The present study reveals that MK615 also exerts hepatoprotective activity in a rat model of D-GalN-induced hepatopathy, given that treatment with MK615 resulted in lower plasma ALT and AST levels accompanied by histological evidence of suppressed destruction of hepatic parenchymal cells when compared with untreated controls. Therefore, MK615 protected the rats from D-GalN-induced hepatopathy.

Previous studies using animal models of D-GalN-induced hepatopathy revealed the activation of MAPKs in the liver[13], suggesting that liver protection might be achieved by the induction of HO-1[14] or by the inhibition of NF-κB in Kupffer cells[15]. In the present study, the effects of MK615 in suppressing MAPK phosphorylation, inducing HO-1, and inhibiting NF-κB activation may have protected the rats from D-GalN-induced hepatopathy.

Additionally, it was shown that the intake of Misatol

ME, which contains MK615, lowered the elevated levels of AST and ALT in patients with hepatic impairment. This effect was observed in patients with etiologically different hepatic diseases, i.e., those with hepatitis C and those with NAFLD. No adverse event was associated with the intake of Misatol ME during this study. Furthermore, add-on Misatol ME in combination with UDCA, which had been initiated before the start of Misatol ME intake, resulted in further AST and ALT level reductions in patients with hepatitis C. Moreover, the reduction in ALT levels was also noted in patients who were previously resistant to UDCA therapy.

A major approach to treating HCV infection is antiviral therapy using a combination of IFN and ribavirin[16]. In cases in which the virus cannot be eradicated or IFN is not indicated, it is important to prevent the progression of HCV infection to liver cirrhosis or liver cancer[17]. In practice, the progression of HCV infection to liver fibrosis is accelerated by higher levels of ALT[18-21]. Therefore, when dealing with cases in which virus eradication is difficult, therapeutic interventions that result in lower ALT levels are important for delaying disease progression. In the present study, Misatol ME was shown to significantly reduce ALT levels in patients with chronic hepatitis C, and further reductions in ALT levels were also observed in patients refractory or poorly responsive to UDCA. Given the significance of these findings, Misatol ME warrants further evaluation as a potential treatment for liver disease, including an evaluation of its efficacy during prolonged use. Because Misatol ME is a functional food, conducting the same controlled study to investigate its potential as a medicine was difficult. Nevertheless, the usefulness of Misatol ME as a functional food was clarified. A future investigation is required in which a detailed analysis of the active principal component of Misatol ME should be conducted to elucidate the mechanism underlying its effectiveness as a functional food.

The mechanism underlying the hepatoprotective activity of Misatol ME in patients with chronic hepatitis C appears to involve the anti-inflammatory and antioxidative actions of the MK615 component of Misatol ME. Patients with chronic hepatitis C have high levels of inflammatory cytokines such as TNF-α and IL-6[22-25]. MK615 inhibits the phosphorylation of MAPKs in LPS-stimulated macrophage-like RAW264.7 cells and suppresses the formation of TNF-α and IL-6 by inhibiting NF-κB activation[12]; these findings suggest that the effect of MK615 in suppressing cytokine formation contributes to the suppression of hepatocyte damage in patients with hepatic impairment. Given that Nrf2 activation[26-29] and HO-1 induction[14,30-32] are known to be hepatoprotective, the authors previously demonstrated that MK615 and its component OA activate the transcription factor Nrf2 in LPS-stimulated macrophage-like RAW264.7 cells and induce HO-1, one of the target genes[3]. Whether MK615 also activates Nrf2 and induces HO-1 in clinical cases is unknown. However, it appears highly probable that the antioxidative action of MK615 protects the liver.

MK615 was also effective in patients with NAFLD, reducing serum AST and ALT levels in these patients, as well as in those with hepatitis C. The involvement of factors such as oxidative stress, insulin resistance, and TNF-α in the progression of NAFLD into non-alcoholic steatohepatitis (NASH) has been suggested[33-35]. Diet and exercise are the standard therapies for the treatment of such cases[36,37]. However, the outcomes of these treatments are often unsatisfactory. The effects of MK615 on oxidative stress and insulin resistance in patients with NAFLD are most likely based on the antioxidative effect and the inflammatory cytokine-suppressive action of MK615. Therefore, MK615 therapy may be a promising new means of treating such cases clinically. Obesity is considered a major factor associated with NAFLD. The livers of obese individuals display disturbances in autophagy, with upregulation of autophagy reducing insulin resistance[38]. Since MK615 has been demonstrated to induce autophagy in colorectal carcinoma cell lines[9], this effect is also expected to be useful for treatment[39]. More recently, it was reported that a rat model of NASH exhibited increased expression of RAGE in the liver, suggesting that inhibiting RAGE expression can protect the liver[40]. MK615 reduces the expression of RAGE on the cell membranes of the high-RAGE expression hepatocellular carcinoma cell line HuH7[8]. This RAGE suppression may also play a role in the hepatoprotective effects of Misatol ME.

In the present study, MK615 and Misatol ME, which contains MK615, were shown to potentially alleviate various types of hepatic impairment caused by different factors. MK615 contains multiple triterpenoids (OA, UA, lupeol, *etc.*); previous in vitro and in vivo studies have shown that these triterpenoids protect the liver from various hepatotoxic substances, such as D-galactosamine, acetaminophen, carbon tetrachloride, and ethanol[27-29,41-47]. As a result of these diverse actions, Misatol ME may exert extensive hepatoprotective effects in patients with hepatic impairments of differing etiologies. Therefore, further studies are required to elucidate the diverse actions of Misatol ME and to assess the significance of its long-term use and its clinical efficacy in suppressing the onset and progression of cancer, as previously demonstrated at experimental level.

COMMENTS

Background

MK615, an extract from Japanese apricot, contains triterpenoids. These substances have been shown to exert various biological actions. In the present study, MK615 (a beverage containing MK615, an *ume* extract) was found to protect hepatocytes from D-galactosamine hydrochloride-induced cytotoxicity in rats. MK615 decreased the elevated alanine aminotransferase (ALT) and aspartate aminotransferase levels in the patients with liver disorder.

Research frontiers

The mechanism underlying the hepatoprotective activity of MK615 in patients with chronic hepatitis C appears to involve the anti-inflammatory and antioxidative actions of the MK615 component of MK615.

Innovations and breakthroughs

This is the first study to indicate that MK615 lowers blood transaminase levels in patients with liver disorders such as chronic hepatitis C and non-alcoholic

fatty liver disease.

Applications

In treating hepatitis C virus infection, therapeutic interventions that result in lower ALT levels are important for delaying disease progression. In the present study, MK615 was shown to significantly reduce the ALT levels in the patients with chronic hepatitis C, and further reductions in ALT levels were observed in the patients refractory or poorly responsive to ursodeoxycholic acid. Given the significance of these findings, MK615 warrants further evaluation as a potential treatment for liver disease, including an evaluation of its efficacy during prolonged use.

Terminology

MK615, an extract from Japanese apricot, contains triterpenoids such as ursolic acid, oleanolic acid, lupeol, α-amyrin, and -sitosterol. *Ume* extracts exert anti-inflammatory and antioxidative actions.

Peer review

The strongest point of this study should be the histological comparison of the rat livers with galactosamine-induced injury pretreated with MK615 and those not pretreated with MK615. The result is interesting and suggest that MK615 are promising hepatoprotective agents for patients with liver disorders.

REFERENCES

1 **Miyazawa M**, Utsunomiya H, Inada K, Yamada T, Okuno Y, Tanaka H, Tatematsu M. Inhibition of Helicobacter pylori motility by (+)-Syringaresinol from unripe Japanese apricot. *Biol Pharm Bull* 2006; **29**: 172-173

2 **Yamai H**, Sawada N, Yoshida T, Seike J, Takizawa H, Kenzaki K, Miyoshi T, Kondo K, Bando Y, Ohnishi Y, Tangoku A. Triterpenes augment the inhibitory effects of anticancer drugs on growth of human esophageal carcinoma cells in vitro and suppress experimental metastasis in vivo. *Int J Cancer* 2009; **125**: 952-960

3 **Kawahara K**, Hashiguchi T, Masuda K, Saniabadi AR, Kikuchi K, Tancharoen S, Ito T, Miura N, Morimoto Y, Biswas KK, Nawa Y, Meng X, Oyama Y, Takenouchi K, Shrestha B, Sameshima H, Shimizu T, Adachi T, Adachi M, Maruyama I. Mechanism of HMGB1 release inhibition from RAW264.7 cells by oleanolic acid in Prunus mume Sieb. et Zucc. *Int J Mol Med* 2009; **23**: 615-620

4 **Al-Jahdari WS**, Sakurai H, Yoshida Y, Mobaraki A, Suzuki Y, Nakano T. MK615, a prospective anti-proliferative agent, enhances CD4/CD8 ratio after exposure to irradiation. *Int J Radiat Biol* 2011; **87**: 81-90

5 **Adachi M**, Suzuki Y, Mizuta T, Osawa T, Adachi T, Osaka K, Suzuki K, Shiojima K, Arai Y, Masuda K, Uchiyama M, Oyamada T, Clerici M. The "Prunus mume Sieb. et Zucc" (Ume) is a Rich Natural Source of Novel Anti-Cancer Substance. *Int J Food Prop* 2007; **10**: 375-384

6 **Nakagawa A**, Sawada T, Okada T, Ohsawa T, Adachi M, Kubota K. New antineoplastic agent, MK615, from UME (a Variety of) Japanese apricot inhibits growth of breast cancer cells in vitro. *Breast J* 2007; **13**: 44-49

7 **Okada T**, Sawada T, Osawa T, Adachi M, Kubota K. A novel anti-cancer substance, MK615, from ume, a variety of Japanese apricot, inhibits growth of hepatocellular carcinoma cells by suppressing Aurora A kinase activity. *Hepatogastroenterology* 2007; **54**: 1770-1774

8 **Sakuraoka Y**, Sawada T, Okada T, Shiraki T, Miura Y, Hiraishi K, Ohsawa T, Adachi M, Takino J, Takeuchi M, Kubota K. MK615 decreases RAGE expression and inhibits TAGE-induced proliferation in hepatocellular carcinoma cells. *World J Gastroenterol* 2010; **16**: 5334-5341

9 **Mori S**, Sawada T, Okada T, Ohsawa T, Adachi M, Keiichi K. New anti-proliferative agent, MK615, from Japanese apricot "Prunus mume" induces striking autophagy in colon cancer cells in vitro. *World J Gastroenterol* 2007; **13**: 6512-6517

10 **Okada T**, Sawada T, Osawa T, Adachi M, Kubota K. MK615 inhibits pancreatic cancer cell growth by dual inhibition of Aurora A and B kinases. *World J Gastroenterol* 2008; **14**: 1378-1382

11 **Matsushita S**, Tada K, Kawahara K, Kawai K, Hashiguchi T, Maruyama I, Kanekura T. Advanced malignant melanoma responds to Prunus mume Sieb. Et Zucc (Ume) extract: Case report and in vitro study. *Exp and Ther Med* 2010; **1**: 569-574

12 **Morimoto Y**, Kikuchi K, Ito T, Tokuda M, Matsuyama T, Noma S, Hashiguchi T, Torii M, Maruyama I, Kawahara K. MK615 attenuates Porphyromonas gingivalis lipopolysaccharide-induced pro-inflammatory cytokine release via MAPK inactivation in murine macrophage-like RAW264.7 cells. *Biochem Biophys Res Commun* 2009; **389**: 90-94

13 **Nishioka H**, Kishioka T, Iida C, Fujii K, Ichi I, Kojo S. Activation of mitogen activated protein kinase (MAPK) during D-galactosamine intoxication in the rat liver. *Bioorg Med Chem Lett* 2006; **16**: 3019-3022

14 **Wen T**, Wu ZM, Liu Y, Tan YF, Ren F, Wu H. Upregulation of heme oxygenase-1 with hemin prevents D-galactosamine and lipopolysaccharide-induced acute hepatic injury in rats. *Toxicology* 2007; **237**: 184-193

15 **Hoffmann F**, Sass G, Zillies J, Zahler S, Tiegs G, Hartkorn A, Fuchs S, Wagner J, Winter G, Coester C, Gerbes AL, Vollmar AM. A novel technique for selective NF-kappaB inhibition in Kupffer cells: contrary effects in fulminant hepatitis and ischaemia-reperfusion. *Gut* 2009; **58**: 1670-1678

16 **Fried MW**, Shiffman ML, Reddy KR, Smith C, Marinos G, Gonçales FL, Häussinger D, Diago M, Carosi G, Dhumeaux D, Craxi A, Lin A, Hoffman J, Yu J. Peginterferon alfa-2a plus ribavirin for chronic hepatitis C virus infection. *N Engl J Med* 2002; **347**: 975-982

17 **Fassio E**. Hepatitis C and hepatocellular carcinoma. *Ann Hepatol* 2010; **9** Suppl: 119-122

18 **Tarao K**, Rino Y, Ohkawa S, Shimizu A, Tamai S, Miyakawa K, Aoki H, Imada T, Shindo K, Okamoto N, Totsuka S. Association between high serum alanine aminotransferase levels and more rapid development and higher rate of incidence of hepatocellular carcinoma in patients with hepatitis C virus-associated cirrhosis. *Cancer* 1999; **86**: 589-595

19 **Toyoda H**, Kumada T, Kiriyama S, Sone Y, Tanikawa M, Hisanaga Y, Hayashi K, Honda T, Kuzuya T. Influence of age, sex, and degree of liver fibrosis on the association between serum alanine aminotransferase levels and liver inflammation in patients with chronic hepatitis C. *Dig Dis Sci* 2004; **49**: 295-299

20 **Rino Y**, Tarao K, Morinaga S, Ohkawa S, Miyakawa K, Hirokawa S, Masaki T, Tarao N, Yukawa N, Saeki H, Takanashi Y, Imada T. Reduction therapy of alanine aminotransferase levels prevent HCC development in patients with HCV-associated cirrhosis. *Anticancer Res* 2006; **26**: 2221-2226

21 **Kurokawa M**, Hiramatsu N, Oze T, Mochizuki K, Yakushijin T, Kurashige N, Inoue Y, Igura T, Imanaka K, Yamada A, Oshita M, Hagiwara H, Mita E, Ito T, Inui Y, Hijioka T, Yoshihara H, Inoue A, Imai Y, Kato M, Kiso S, Kanto T, Takehara T, Kasahara A, Hayashi N. Effect of interferon alpha-2b plus ribavirin therapy on incidence of hepatocellular carcinoma in patients with chronic hepatitis. *Hepatol Res* 2009; **39**: 432-438

22 **Nelson DR**, Lim HL, Marousis CG, Fang JW, Davis GL, Shen L, Urdea MS, Kolberg JA, Lau JY. Activation of tumor necrosis factor-alpha system in chronic hepatitis C virus infection. *Dig Dis Sci* 1997; **42**: 2487-2494

23 **Gochee PA**, Jonsson JR, Clouston AD, Pandeya N, Purdie DM, Powell EE. Steatosis in chronic hepatitis C: association with increased messenger RNA expression of collagen I, tumor necrosis factor-alpha and cytochrome P450 2E1. *J Gastroenterol Hepatol* 2003; **18**: 386-392

24 **Malaguarnera M**, Di Fazio I, Romeo MA, Restuccia S, Laurino A, Trovato BA. Elevation of interleukin 6 levels in patients with chronic hepatitis due to hepatitis C virus. *J Gastroenterol* 1997; **32**: 211-215

25 **Oyanagi Y**, Takahashi T, Matsui S, Takahashi S, Boku S, Takahashi K, Furukawa K, Arai F, Asakura H. Enhanced

expression of interleukin-6 in chronic hepatitis C. *Liver* 1999; **19**: 464-472
26 **Okada K**, Shoda J, Taguchi K, Maher JM, Ishizaki K, Inoue Y, Ohtsuki M, Goto N, Takeda K, Utsunomiya H, Oda K, Warabi E, Ishii T, Osaka K, Hyodo I, Yamamoto M. Ursodeoxycholic acid stimulates Nrf2-mediated hepatocellular transport, detoxification, and antioxidative stress systems in mice. *Am J Physiol Gastrointest Liver Physiol* 2008; **295**: G735-G747
27 **Liu J**, Wu Q, Lu YF, Pi J. New insights into generalized hepatoprotective effects of oleanolic acid: key roles of metallothionein and Nrf2 induction. *Biochem Pharmacol* 2008; **76**: 922-928
28 **Reisman SA**, Aleksunes LM, Klaassen CD. Oleanolic acid activates Nrf2 and protects from acetaminophen hepatotoxicity via Nrf2-dependent and Nrf2-independent processes. *Biochem Pharmacol* 2009; **77**: 1273-1282
29 **Wang X**, Ye XL, Liu R, Chen HL, Bai H, Liang X, Zhang XD, Wang Z, Li WL, Hai CX. Antioxidant activities of oleanolic acid in vitro: possible role of Nrf2 and MAP kinases. *Chem Biol Interact* 2010; **184**: 328-337
30 **Zhu Z**, Wilson AT, Mathahs MM, Wen F, Brown KE, Luxon BA, Schmidt WN. Heme oxygenase-1 suppresses hepatitis C virus replication and increases resistance of hepatocytes to oxidant injury. *Hepatology* 2008; **48**: 1430-1439
31 **Roller J**, Laschke MW, Scheuer C, Menger MD. Heme oxygenase (HO)-1 protects from lipopolysaccharide (LPS)-mediated liver injury by inhibition of hepatic leukocyte accumulation and improvement of microvascular perfusion. *Langenbecks Arch Surg* 2010; **395**: 387-394
32 **Immenschuh S**, Baumgart-Vogt E, Mueller S. Heme oxygenase-1 and iron in liver inflammation: a complex alliance. *Curr Drug Targets* 2010; **11**: 1541-1550
33 **Day CP**, James OF. Steatohepatitis: a tale of two "hits"? *Gastroenterology* 1998; **114**: 842-845
34 **Ekstedt M**, Franzén LE, Mathiesen UL, Thorelius L, Holmqvist M, Bodemar G, Kechagias S. Long-term follow-up of patients with NAFLD and elevated liver enzymes. *Hepatology* 2006; **44**: 865-873
35 **Tomita K**, Tamiya G, Ando S, Ohsumi K, Chiyo T, Mizutani A, Kitamura N, Toda K, Kaneko T, Horie Y, Han JY, Kato S, Shimoda M, Oike Y, Tomizawa M, Makino S, Ohkura T, Saito H, Kumagai N, Nagata H, Ishii H, Hibi T. Tumour necrosis factor alpha signalling through activation of Kupffer cells plays an essential role in liver fibrosis of non-alcoholic steatohepatitis in mice. *Gut* 2006; **55**: 415-424
36 **Suzuki A**, Lindor K, St Saver J, Lymp J, Mendes F, Muto A, Okada T, Angulo P. Effect of changes on body weight and lifestyle in nonalcoholic fatty liver disease. *J Hepatol* 2005; **43**: 1060-1066
37 **Omagari K**, Morikawa S, Nagaoka S, Sadakane Y, Sato M, Hamasaki M, Kato S, Masuda J, Osabe M, Kadota T, Sera K. Predictive factors for the development or regression of Fatty liver in Japanese adults. *J Clin Biochem Nutr* 2009; **45**: 56-67
38 **Rautou PE**, Mansouri A, Lebrec D, Durand F, Valla D, Moreau R. Autophagy in liver diseases. *J Hepatol* 2010; **53**: 1123-1134
39 **Amir M**, Czaja MJ. Autophagy in nonalcoholic steatohepatitis. *Expert Rev Gastroenterol Hepatol* 2011; **5**: 159-166
40 **Wu J**, Zhao MY, Zheng H, Zhang H, Jiang Y. Pentoxifylline alleviates high-fat diet-induced non-alcoholic steatohepatitis and early atherosclerosis in rats by inhibiting AGE and RAGE expression. *Acta Pharmacol Sin* 2010; **31**: 1367-1375
41 **Liu J**, Liu Y, Klaassen CD. Protective effect of oleanolic acid against chemical-induced acute necrotic liver injury in mice. *Zhongguo Yao Li Xue Bao* 1995; **16**: 97-102
42 **Liu Y**, Kreppel H, Liu J, Choudhuri S, Klaassen CD. Oleanolic acid protects against cadmium hepatotoxicity by inducing metallothionein. *J Pharmacol Exp Ther* 1993; **266**: 400-406
43 **Liu J**, Liu Y, Madhu C, Klaassen CD. Protective effects of oleanolic acid on acetaminophen-induced hepatotoxicity in mice. *J Pharmacol Exp Ther* 1993; **266**: 1607-1613
44 **Tang XH**, Gao J, Fang F, Chen J, Xu LZ, Zhao XN, Xu Q. Hepatoprotection of oleanolic acid is related to its inhibition on mitochondrial permeability transition. *Am J Chin Med* 2005; **33**: 627-637
45 **Saravanan R**, Viswanathan P, Pugalendi KV. Protective effect of ursolic acid on ethanol-mediated experimental liver damage in rats. *Life Sci* 2006; **78**: 713-718
46 **Martin-Aragón S**, de las Heras B, Sanchez-Reus MI, Benedi J. Pharmacological modification of endogenous antioxidant enzymes by ursolic acid on tetrachloride-induced liver damage in rats and primary cultures of rat hepatocytes. *Exp Toxicol Pathol* 2001; **53**: 199-206
47 **Sunitha S**, Nagaraj M, Varalakshmi P. Hepatoprotective effect of lupeol and lupeol linoleate on tissue antioxidant defence system in cadmium-induced hepatotoxicity in rats. *Fitoterapia* 2001; **72**: 516-523

S- Editor Gou SX **L- Editor** A **E- Editor** Zhang DN

GASTROENTEROLOGY 2012;142:366–376

CCR9$^+$ Macrophages Are Required for Acute Liver Inflammation in Mouse Models of Hepatitis

NOBUHIRO NAKAMOTO,* HIROTOSHI EBINUMA,* TAKANORI KANAI,* PO-SUNG CHU,* YUICHI ONO,* YOHEI MIKAMI,* KEISUKE OJIRO,* MARTIN LIPP,‡ PAUL E. LOVE,§ HIDETSUGU SAITO,* and TOSHIFUMI HIBI*

*Division of Gastroenterology and Hepatology, Department of Internal Medicine, Keio University School of Medicine, Tokyo, Japan; ‡Department of Tumor Genetics and Immunogenetics, Max-Delbruck Center for Molecular Medicine, Berlin, Germany; and §Laboratory of Mammalian Genes and Development, National Institute of Child Health and Human Development, National Institutes of Health, Bethesda, Maryland

BACKGROUND & AIMS: Antigen-presenting cells (APCs) are involved in the induction of liver inflammation. We investigated the roles of specific APCs in the pathogenesis of acute liver injury in mice. **METHODS:** We used concanavalin A (con A) or carbon tetrachloride to induce acute liver inflammation in mice and studied the roles of macrophages that express CCR9. **RESULTS:** After injection of con A, we detected CCR9$^+$CD11b$^+$CD11c$^-$ macrophages that express tumor necrosis factor (TNF)-α in livers of mice, whereas CCR9$^+$Siglec-H$^+$CD11b$^-$ CD11c^{low} plasmacytoid DCs (pDCs), which are abundant in normal livers, disappeared. The CCR9$^+$ macrophages were also detected in the livers of *RAG-2*$^{-/-}$ mice, which lack lymphocytes and natural killer T cells, after injection of con A. Under inflammatory conditions, CCR9$^+$ macrophages induced naive CD4$^+$ T cells to become interferon gamma–producing Th1 cells in vivo and in vitro. *CCR9*$^{-/-}$ mice injected with con A did not develop hepatitis unless they also received CCR9$^+$ macrophages from mice that received con A; more CCR9$^+$ macrophages accumulated in their inflamed livers than CCR9$^+$ pDCs, CCR9$^-$ pDCs, or CCR9$^-$ macrophages isolated from mice that had received injections of con A. Levels of *CCL25* messenger RNA increased in livers after injection of con A; neutralizing antibodies against CCL25 reduced the induction of hepatitis by con A by blocking the migration of CCR9$^+$ macrophages and their production of TNF-α. Peripheral blood samples from patients with acute hepatitis had greater numbers of TNF-α–producing CCR9$^+$CD14$^+$ CD16^{high} monocytes than controls. **CONCLUSIONS: CCR9$^+$ macrophages contribute to the induction of acute liver inflammation in mouse models of hepatitis.**

Keywords: Immune Regulation; Hepatic Disease; Chemokine Receptor; T-Cell Activation.

BASIC AND TRANSLATIONAL LIVER

Although the liver faces continuous exposure to many pathogens and commensal bacterial products, the innate and adaptive immune responses of the liver favor the induction of immunologic tolerance.[1–5] Critically, however, there are many patients who experience acute hepatic failure, with a high lethal rate owing to liver inflammation.[6] Although various immune compartments, such as T cells including CD4$^+$CD25$^+$Foxp3$^+$ regulatory T cells, natural killer cells, natural killer T (NKT) cells, macrophages (Kupffer cells), conventional DCs (cDCs), and plasmacytoid DCs (pDCs), reside in the normal liver,[1,2] it is unknown which types of cells positively induce inflammation.

Accumulating evidence shows that the chemokine/chemokine receptor axis instructs immune cells into the inflamed liver.[7] Originally, CCR9 is a representative gut-homing receptor on lymphocytes that migrate into the small intestine, where CCL25 (ligand of CCR9) is abundant.[8] Furthermore, up-regulation of CCL25 in the inflamed small intestine following accumulation of CCR9$^+$ CD4$^+$ T cells has been reported both in Crohn's disease[9] and in a murine model,[10,11] and clinical trials of anti-CCR9 antagonist against Crohn's disease are ongoing. In liver immunology, however, Eksteen et al previously showed that CCL25 is up-regulated in the inflamed liver of primary sclerosing cholangitis in humans and that CCR9-expressing T cells are accumulated in the liver of such patients.[12] Although initial studies focused on CCR9-expressing lymphocytes irrespective of the gut and liver, Hadeiba et al recently showed that immature pDCs in the spleen and lymph nodes also express CCR9 and that those CCR9-expressing pDCs have the ability to suppress immune responses.[13] However, little is known of the function of CCR9-expressing pDCs in the liver and also of the presence and the function of liver CCR9-expressing macrophages and cDCs.

To examine the induction of liver inflammation, we compared 2 typical conditions—the steady condition versus the inflammatory condition—using an acute T cell–mediated hepatitis model, concanavalin A (con A)–induced liver inflammation in mice,[14] focusing on antigen-presenting cells (APCs)[15–18] and the chemokine/chemokine receptor axis.[7] Intravenous injection of con A induces massive hepatocyte necrosis, with marked infil-

Abbreviations used in this paper: AH, acute hepatitis; APC, antigen-presenting cell; CH, chronic hepatitis; cDC, conventional dendritic cell; con A, concanavalin A; GAPDH, glyceraldehyde-3-phosphate dehydrogenase; IFN, interferon; IL, interleukin; mAb, monoclonal antibody; NC, normal control; NKT, natural killer T; PB, peripheral blood; pDC, plasmacytoid dendritic cell; TLR, Toll-like receptor; TNF, tumor necrosis factor; WT, wild-type.

0016-5085/$36.00
doi:10.1053/j.gastro.2011.10.039

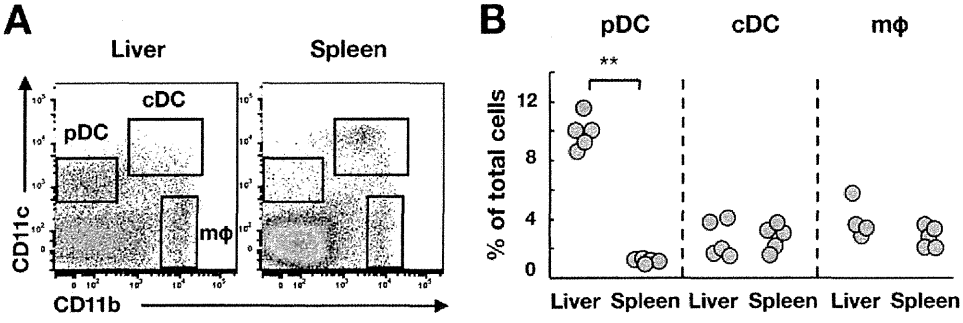

Figure 1. Abundant CCR9$^+$CD11b$^-$CD11c^{low} pDCs in the normal liver. (*A*) Representative CD11b and CD11c staining on whole cells isolated from the liver and spleen of WT mice. Each *box* indicates cDCs, CD11b$^+$CD11c$^+$; pDCs, CD11b$^-$CD11c^{low}; and macrophages, CD11b$^+$CD11c$^-$. (*B*) Mean percentage of pDCs, cDCs, and macrophages. Data show mean ± SEM (n = 5/group). $^{**}P < .01$.

tration of lymphocytes in the liver and elevation of serum transaminase levels. Initially, this model was believed to be CD4$^+$ T-cell dependent; later, however, 2 groups clarified that the pathologic CD4$^+$ T cells were CD1d-dependent NKT cells.[19,20] Against this background, we here propose that liver CCR9$^+$ macrophages act specifically as initial inflammatory cells in the development of con A–induced T-cell hepatitis.

Materials and Methods

Experimental Protocols of con A–Induced Hepatitis

Con A (type IV) was purchased from Sigma-Aldrich (St Louis, MO). Intravenous injections of con A (20 mg/kg) were administered into the tail vein of mice 12 hours before examination under anesthesia. In experiment 1, age-matched wild-type (WT), *CCR9*$^{-/-}$, *CCR7*$^{-/-}$, and *MCP-1*$^{-/-}$ mice were treated with con A. In experiment 2, CCR9$^+$ and CCR9$^-$ macrophages as well as CCR9$^+$ and CCR9$^-$ pDCs were isolated from the liver of con A–treated Ly5.1$^+$ mice. These cells were then adoptively transferred to *CCR9*$^{-/-}$ Ly5.2$^+$ mice (5×10^5 cells/mice), which were immediately injected with con A. As a control, WT Ly5.2$^+$ mice were injected with con A. In experiment 3, WT mice were intraperitoneally injected with neutralizing anti-CCL25 monoclonal antibody (mAb) (500 μg/mouse, clone 89818; R&D Systems, Minneapolis, MN; n = 4) or isotype control (n = 4) 2 hours before administration of con A. All mice were killed 12 hours after administration of con A.

See Supplementary Materials and Methods for more details.

Results

Abundant CCR9$^+$CD11b$^-$CD11c^{low} pDCs in the Normal Liver

To clarify the mechanism by which liver inflammation is induced, we focused on liver APCs.[1,2,15,16] To segmentalize the APC compartments, we stained liver and spleen mononuclear cells obtained from WT mice with mAb against CD11b and CD11c. As shown in Figure 1*A*, 3 APC compartments were found in the liver and spleen: cDCs, CD11b$^+$CD11c$^+$; pDCs, CD11b$^-$CD11c^{low}; and macrophages, CD11b$^+$CD11c$^-$. As previously reported,[1] pDCs are more abundant in the liver than in the spleen, although the ratios of cDCs to macrophages were comparable in these organs (Figure 1*B*). To further characterize these compartments, we stained the cells with a third mAb (Supplementary Figure 1). Consistent with previous reports,[13,21] B220, PDCA-1, CCR9, and CD8α were preferentially expressed on pDCs but not on cDCs or macrophages in liver and spleen cells. However, not all CD11b$^-$CD11c^{low} cells appeared to be identical to pDCs because some of the latter cells did not express the markers. Interestingly, the liver pDC population contained a higher proportion of CCR9$^+$ cells than spleen pDCs, which suggests that liver pDCs are more immature and tolerogenic than spleen pDCs.[13,21] In contrast, F4/80 was expressed not only on spleen and liver macrophages, but also on liver cDCs and some spleen cDCs. This implies that macrophages in the liver and spleen and cDCs in the liver can be classified exclusively as monocyte phagocyte system[15] cells generated from monocytes and also that spleen cDCs are a mixture of macrophage/dendritic precursor- and monocyte-derived DCs.[16] In this regard, macrophages and cDCs in the liver and spleen expressed Ly6C at a high level and a low to negative level, respectively. CD80, CD86, and major histocompatibility complex class II on liver and spleen cells were expressed at a high level on cDCs but at moderate to low levels on macrophages and pDCs (Supplementary Figure 1). Collectively, these data suggest that pDCs and cDCs/macrophages are distinct populations in the liver, whereas cDCs and macrophages constitute similar but different populations in terms of activation status.

Accumulation of CCR9-Expressing Macrophages Through con A–Induced Liver Inflammation

To induce liver inflammation, we intravenously administered con A to WT mice. Twelve hours after administration, the APC compartments in the liver showed marked changes; the proportion of pDCs was significantly reduced, whereas that of cDCs/macrophages, particularly macrophages, was significantly increased (Figure 2*Ai* and *Bi*). In contrast, the APC composition of spleen cells was unchanged by administration of con A (Figure 2*Ai* and *Bi*). Consistent with these findings, the absolute cell numbers of cDCs and macrophages in the liver were signifi-

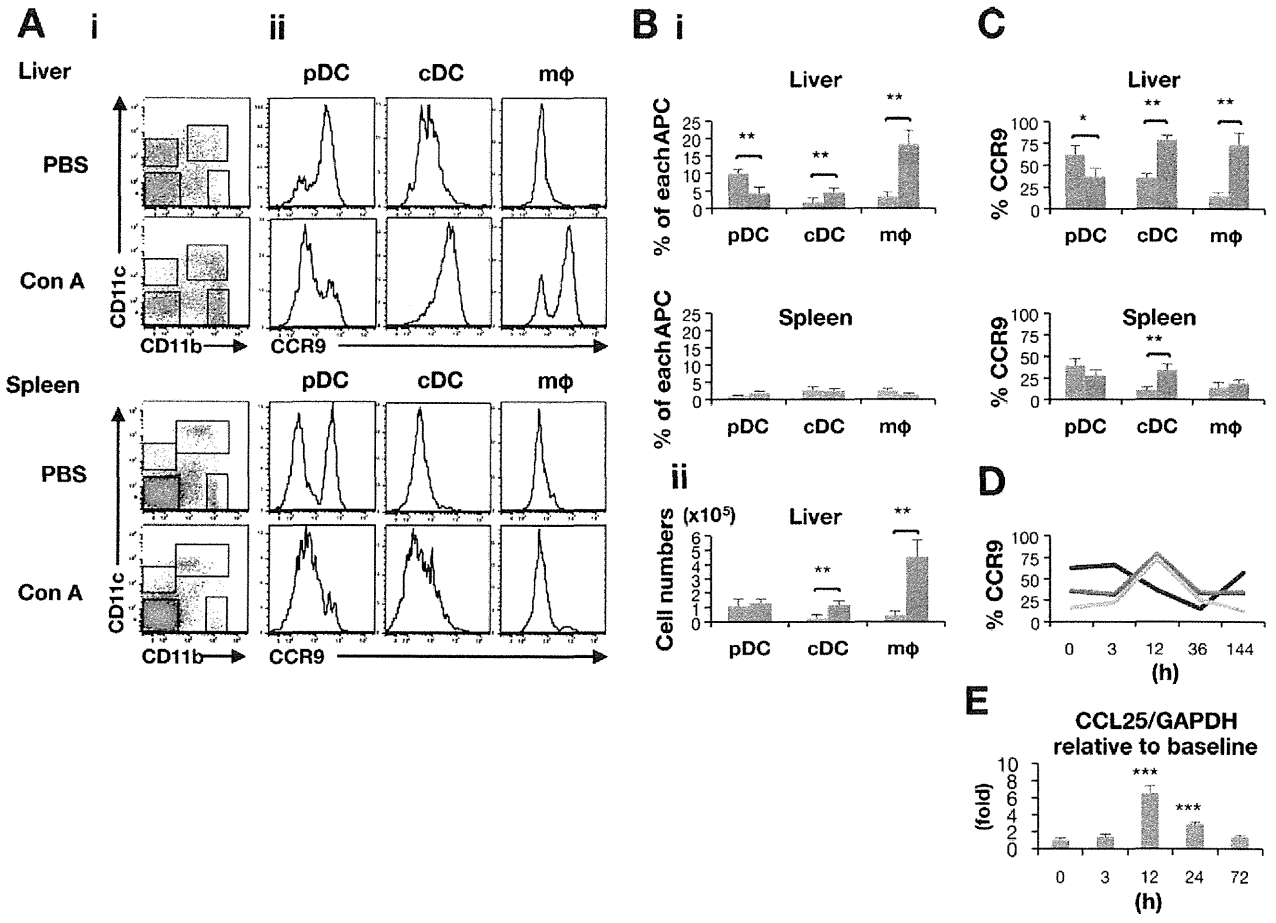

Figure 2. Accumulation of CCR9-expressing macrophages in the liver of con A–treated mice. (*Ai*) CD11b and CD11c staining on whole cells in the liver and spleen from PBS- or con A–treated mice. (*Aii*) CCR9 staining for the gated APCs. Data are representative of 5 independent experiments. (*Bi*) Mean percentages in 3 subsets of the liver (*upper panel*) and spleen (*middle panel*) and (*Bii*) absolute cell numbers of the 3 subsets of the liver (*lower panel*). Data show mean ± SEM (n = 5/group). *Blue bars*, PBS; *red bars*, con A. $^{**}P < .01$. (*C*) Mean percentages of CCR9$^+$ cells in the 3 subsets of the liver (*upper panel*) or spleen (*lower panel*). *Blue bars*, PBS; *red bars*, con A. $^{*}P < .05$, $^{**}P < .01$. (*D*) Time course changes of mean percentages of CCR9$^+$ cells in the 3 subsets of the liver after con A injection. *Blue line*, pDCs; *red line*, cDCs; *green line*, macrophages. Data show mean ± SEM (n = 4/group). (*E*) CCL25 expression in the liver after con A injection. CCL25 mRNA expression in the livers of PBS- and con A–treated mice was measured by reverse-transcription quantitative polymerase chain reaction, and each sample was normalized relative to glyceraldehyde-3-phosphate dehydrogenase (GAPDH) expression. *Error bars* represent SEM of triplicate samples. $^{***}P < .001$.

cantly higher in con A–treated mice, whereas those of pDCs were comparable in phosphate-buffered saline (PBS)- and con A–treated mice (Figure 2*Bii*). Surprisingly, we found a dramatic change in CCR9 expression in the liver, but not in the spleen, after administration of con A: down-regulation on pDCs and a corresponding up-regulation on macrophages/cDCs (Figure 2*Aii* and *C*). This change was confirmed by time course observation of CCR9 expression after administration of con A (Figure 2*D*). Furthermore, the expression level of CCL25 messenger RNA (mRNA) in the liver of con A–treated mice was significantly up-regulated 12 hours after injection of con A (Figure 2*E*).

Interestingly, not only did macrophages/cDCs in the liver of con A–treated mice show markedly up-regulated CD80 and CD86 expression compared with those in the liver of PBS-treated mice, but also the mean fluorescent intensity of CD80 and CD86 expression of CCR9$^+$ macrophages/cDCs was significantly higher than in CCR9$^-$ macrophages/cDCs (Supplementary Figure 2*A* and *B*). In contrast, although both CCR9$^-$ and CCR9$^+$ pDCs in the liver of PBS-injected mice were in the CD80$^-$ and CD86$^-$ population, only CCR9$^-$ pDCs in the liver of con A–treated mice showed up-regulated CD80 and CD86 expression (Supplementary Figure 2*A*). Notably, CCR9$^+$ macrophages/cDCs, but not pDCs, expressed a significantly higher level of tumor necrosis factor (TNF)-α after injection of con A (Supplementary Figure 2*C* and *D*). The phenotypic difference between CCR9$^+$ pDCs in the steady state and CCR9$^+$ macrophages under inflammation was also confirmed in that only the CCR9$^+$ pDC population, not CCR9$^+$ macrophages, coexpressed the specific pDC marker Siglec-H[22,23] (Supplementary Figure 2*E*). Furthermore, in vitro stimulation with con A slightly up-regulated CCR9 expression on CD11b$^+$ macrophages of the spleen and liver at 12 and 24 hours after culture. Marked up-regulation was

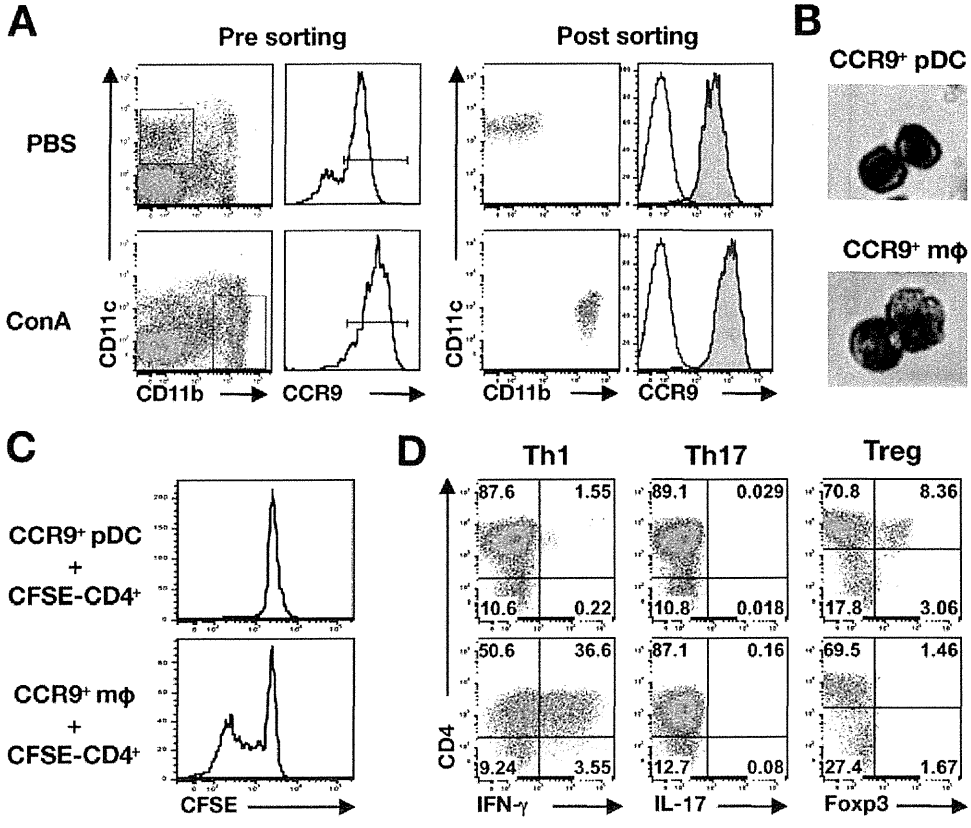

Figure 3. CCR9+ macrophages in the livers of con A–treated mice promote the development of Th1 cells. (*A*) Gating strategy applied to sort CCR9+ pDCs and macrophages from the liver of PBS- and con A–treated mice, respectively. (*B*) Morphology of Giemsa-stained CCR9+ pDCs or CCR9+ macrophages. Data are representative of 2 independent experiments. (*C*) Proliferation of carboxyfluorescein succinimidyl ester (CFSE)-labeled naive CD4+ T cells from *DO11.10* × *RAG-2*$^{-/-}$ mice, cultured for 3 days with CCR9+ pDCs or CCR9+ macrophages in the presence of ovalbumin. Data are representative of 3 independent experiments. (*D*) Intracellular IFN-γ, IL-17A, and Foxp3 expression in CD4+ T cells cultured for 5 days with CCR9+ pDCs (*upper panel*) or CCR9+ macrophages (*lower panel*) in the presence of ovalbumin. Data are representative of 3 independent experiments.

observed only in liver cells at 72 hours after culture (Supplementary Figure 2*F*), although this up-regulated CCR9 expression was less than that induced after in vivo con A administration in mice (Supplementary Figure 2*F*).

We next sought to establish whether the increased CCR9+ macrophages were also observed in the liver of *RAG-2*$^{-/-}$ mice following administration of con A; we wished to determine whether macrophages or T/NKT cells are the primary cells in response to con A in this model. As shown in Supplementary Figure 3*A*, the accumulation of CD11b+CD11c− macrophages and the up-regulation of CCR9 in the macrophages subset were similarly observed in the liver of con A–treated WT and *RAG-2*$^{-/-}$ mice. By contrast, an activated CD69^{high}CD3+ population, including conventional T and NKT cells, was observed in con A–treated WT mice, but it was completely absent in con A–treated *RAG-2*$^{-/-}$ mice. The severity of liver inflammation was dramatically reduced in con A–treated *RAG-2*$^{-/-}$ mice from an assessment of the liver histology and serum levels of transaminase (Supplementary Figure 3*B* and *C*). These results suggest that NKT cells might be terminal effector cells, rather than initiator cells, following the activation of macrophages in a con A hepatitis model.

CCR9+ Macrophages in the Livers From con A–Treated Mice Promote the Development of Th1 Cell

To investigate the function of CCR9+ macrophages in the livers from con A–treated mice (CCR9+ macrophages) in addition to CCR9+ pDCs in the livers from PBS-treated mice (CCR9+ pDCs), both subsets were isolated using FACSAria (BD Biosciences, Franklin Lakes, NJ) (Figure 3*A*) and their morphologic characters were assessed using Giemsa staining. CCR9+ pDCs resembled plasma cells with an eccentric kidney-shaped nucleus, whereas CCR9+ macrophages displayed a horseshoe-shaped nucleus (Figure 3*B*). Next, CCR9+ pDCs or CCR9+ macrophages were cocultured with carboxyfluorescein succinimidyl ester–labeled naive CD4+ T cells obtained from the spleen of *DO11.10* × *RAG-2*$^{-/-}$ mice in the presence of ovalbumin peptides. After 72 hours of culture, CD4+ T cells had extensively divided in the presence of CCR9+ macrophages but showed little division in the presence of CCR9+ pDCs (Figure 3*C*); this finding is consistent with previous reports showing the poor stimulatory function of pDCs.[24,25] We further examined the expression of interferon (IFN)-γ, interleukin (IL)-17A, and Foxp3 in cultured CD4+ T cells. As depicted in Figure 3*D*, CD4+ T cells cocultured with CCR9+ macrophages expressed IFN-γ but not Foxp3 and IL-17A; CD4+ T cells cocultured with CCR9+ pDCs expressed Foxp3 but not IL-17A and IFN-γ.

We next performed a reverse-transcription quantitative polymerase chain reaction assay of the gene expression of CCR9+ macrophages and CCR9+ pDCs. Expression of TNF-α mRNA in CCR9+ macrophages was significantly increased; conversely, that of IL-10 and transforming growth factor β mRNAs in CCR9+ macrophages was significantly decreased (Supplementary Figure 4). Consis-

tent with the findings of a previous report,[26] the expression patterns of Toll-like receptors (TLRs) in CCR9$^+$ macrophages and CCR9$^+$ pDCs were distinct; CCR9$^+$ pDCs preferentially expressed TLR7 and TLR9 mRNAs, whereas CCR9$^+$ macrophages preferentially expressed TLR4 and TLR6 mRNAs (Supplementary Figure 4). This suggests that these 2 populations are separately generated from different precursor cells. Furthermore, the expression of CCR2 mRNA was significantly higher in CCR9$^+$ macrophages; conversely, the expression of CX3CR1 mRNA was significantly lower in CCR9$^+$ macrophages than in CCR9$^+$ pDCs. The expression of CCR5, CCR6, and CCR7 mRNAs was comparable in CCR9$^+$ macrophages and CCR9$^+$ pDCs (Supplementary Figure 4).

CCR9$^{-/-}$ Mice Were Resistant to con A–Induced Hepatitis

To investigate the role of CCR9 during liver inflammation, we used *CCR9$^{-/-}$* mice in a con A–induced hepatitis model. First, the proportion of pDCs in the liver of untreated *CCR9$^{-/-}$* mice was slightly lower than that of untreated WT mice, but the difference was not significant (data not shown). No inflammatory lesions were found in the liver of *CCR9$^{-/-}$* mice until the age of 40 weeks (data not shown). This suggests that CCR9$^+$ pDCs are not the only cells responsible for liver tolerance and inflammation in the steady state and that other CCR9-expressing cells, such as activated CCR9$^+$ macrophages, are needed to induce inflammation. To test this, we administered age-matched WT, *CCR9$^{-/-}$*, *CCR7$^{-/-}$*, and *MCP-1$^{-/-}$* (MCP-1 [CCL2]; CCR2 ligand) mice with con A. As expected, *CCR9$^{-/-}$* mice did not develop liver damage after treatment with con A (Figure 4*B*) and showed less elevation of transaminase levels than the treated WT mice (Figure 4C); con A–treated *CCR7$^{-/-}$* and *MCP-1$^{-/-}$* mice developed hepatitis to a similar extent to con A–treated WT mice (Figure 4*B* and *C*). This suggests that the CCR9/CCL25 axis plays an important role in the pathogenesis of this model. The proportion of macrophages in the liver of *CCR9$^{-/-}$* mice after con A treatment was comparable with that of WT mice treated with PBS, whereas con A–treated WT, *CCR7$^{-/-}$*, and *MCP-1$^{-/-}$* mice showed marked increases of CCR9$^+$ macrophages (Figure 4*A* and *Di*). This was confirmed by the absolute cell numbers of liver CD11b$^+$ macrophages after treatment with con A (Figure 4*Dii*). The diseased WT, *CCR7$^{-/-}$*, and *MCP-1$^{-/-}$* mice showed up-regulation of CCR9 on macrophages and down-regulation on pDCs (Figure 4*E*). Furthermore, we confirmed that the serum levels of TNF-α, IFN-γ, and IL-6 in con A–treated *CCR9$^{-/-}$* mice at 12 hours after administration of con A were significantly reduced compared with those in con A–treated WT mice (Figure 4*F*). Importantly, the activation of NKT and T-cell subsets observed in con A–treated WT mice was diminished in con A–treated *CCR9$^{-/-}$* mice, which suggests that the reciprocal interaction between CCR9-expressing macrophages and NKT/T cells plays a key role in the development of con A–induced acute hepatic inflammation (Supplementary Figure 5). We also confirmed that *CCR9$^{-/-}$* mice were resistant to carbon tetrachloride–induced liver inflammation, another model of acute liver injury in mice, accompanied by the up-regulation of CCR9 expression on CD11b$^+$ macrophages in the liver of carbon tetrachloride–treated WT mice (Supplementary Figure 6).

CCR9$^+$ Macrophages Were Key Inflammatory Cells for con A–Induced T-Cell Hepatitis

Given the evidence that inducible CCR9 expression on macrophages in the liver is crucially involved in the induction of liver inflammation, we further confirmed the direct involvement of CCR9$^+$ macrophages without the possible impact of CCR9$^+$ lymphocytes[12,27] in the T cell–mediated con A model. To this end, CCR9$^+$ and CCR9$^-$ macrophages and CCR9$^+$ and CCR9$^-$ pDCs were isolated from the liver of identically con A–treated Ly5.1$^+$ WT mice, and those cells were then adoptively transferred into Ly5.2$^+$ *CCR9$^{-/-}$* mice, which were immediately injected with con A (Figure 5*A*). As a control, Ly5.2$^+$ WT mice were injected with con A (Figure 5*A*). Strikingly, con A–treated *CCR9$^{-/-}$* mice transferred with CCR9$^+$ macrophages developed more severe hepatitis than mice transferred with CCR9$^+$ pDCs, CCR9$^-$ pDCs, or CCR9$^-$ macrophages from an assessment of the liver histology and serum levels of transaminase (Figure 5*B* and *C*); however, con A–treated *CCR9$^{-/-}$* mice transferred with CCR9$^+$ macrophages showed less liver inflammation than con A–treated WT mice (Figure 5*B* and *C*). Consistent with this, the ratios of CCR9$^+$CD11b$^+$ macrophages were markedly increased in the liver of con A–treated WT mice and *CCR9$^{-/-}$* mice transferred with CCR9$^+$ macrophages, although this was not observed in *CCR9$^{-/-}$* mice transferred with CCR9$^+$ or CCR9$^-$ pDCs or CCR9$^-$ macrophages (Figure 5*D* and *E*). This result suggests a specific role of migrating CCR9$^+$ macrophages as key inflammatory cells in the development of con A–induced hepatitis. Additionally, we confirmed that the increased CCR9$^+$CD11b$^+$ macrophages in con A–treated *CCR9$^{-/-}$* mice transferred with CCR9$^+$ macrophages were Ly5.1$^+$ transferred cells, whereas those in con A–treated WT mice were Ly5.2$^+$ endogenous cells (Figure 5*E*, *right*).

We next investigated whether the transfer of CCR9$^+$ macrophages obtained from con A–treated Ly5.1$^+$ WT mice into *CCR9$^{-/-}$* mice without con A administration could induce liver inflammation (Supplementary Figure 7*A*). As controls, we used *CCR9$^{-/-}$* mice without the transfer or con A administration as well as *CCR9$^{-/-}$* mice with the transfer of CCR9$^+$ macrophages and con A administration (Supplementary Figure 7*A*). However, in sharp contrast to *CCR9$^{-/-}$* mice transferred with CCR9$^+$ macrophages and con A administration, Ly5.1$^+$CD11b$^+$ macrophages were not accumulated in the liver of *CCR9$^{-/-}$* mice transferred with CCR9$^+$ macrophages but without con A administration and in *CCR9$^{-/-}$* mice without the transfer or con A administration (Supplementary Figure 7*B*). Consistent with this, *CCR9$^{-/-}$* mice transferred with CCR9$^+$ macrophages and without con A administration and *CCR9$^{-/-}$* mice without the transfer or con A

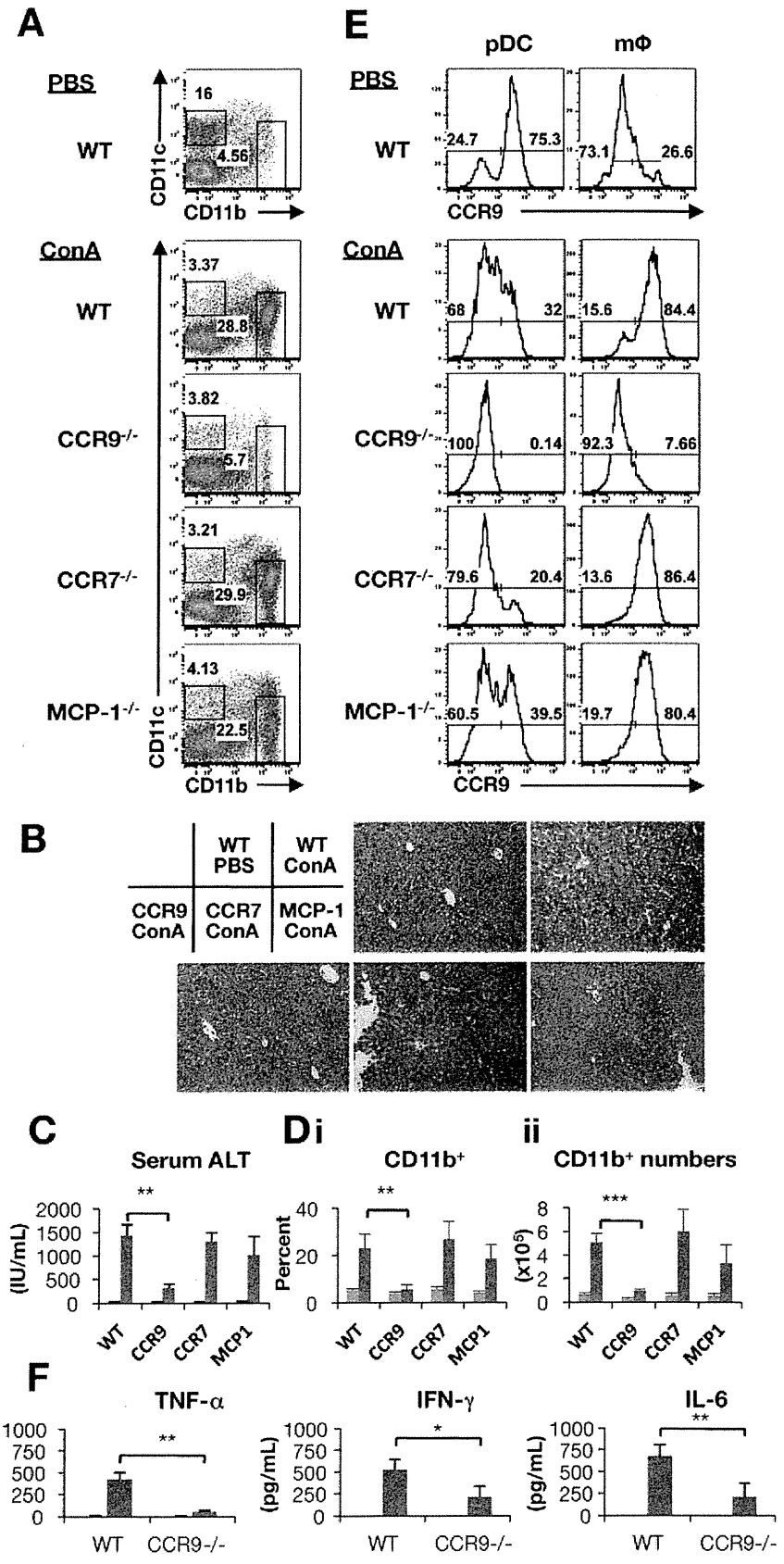

Figure 4. *CCR9*$^{-/-}$ mice are resistant to con A–induced hepatitis. (*A*) CD11b and CD11c staining on whole cells in the liver from PBS- or con A-injected WT, *CCR9*$^{-/-}$, *CCR7*$^{-/-}$, and *MCP-1*$^{-/-}$ mice. Data are representative of 5 independent experiments. (*B*) Photomicrographs of H&E-stained sections of liver. (*C*) Serum ALT level. Data show mean ± SEM (n = 6/group). *Blue bars*, PBS; *red bars*, con A. $^{**}P < .01$. (*Di*) Mean percentage of macrophage subset of the liver and (*Dii*) absolute cell number of macrophages of the liver. Data show mean ± SEM (n = 6/group). *Blue bars*, PBS; *red bars*, con A. $^{**}P < .01$; $^{***}P < .001$. (*E*) CCR9 staining on pDC and macrophage subsets of the liver. Data are representative of 5 independent experiments. (*F*) Serum levels of TNF-α, IFN-γ, and IL-6 from PBS- or con A–treated mice detected by CBA assay. Data show mean ± SEM (n = 4/group). *Red bars*, con A. $^{*}P < .05$; $^{**}P < .01$.

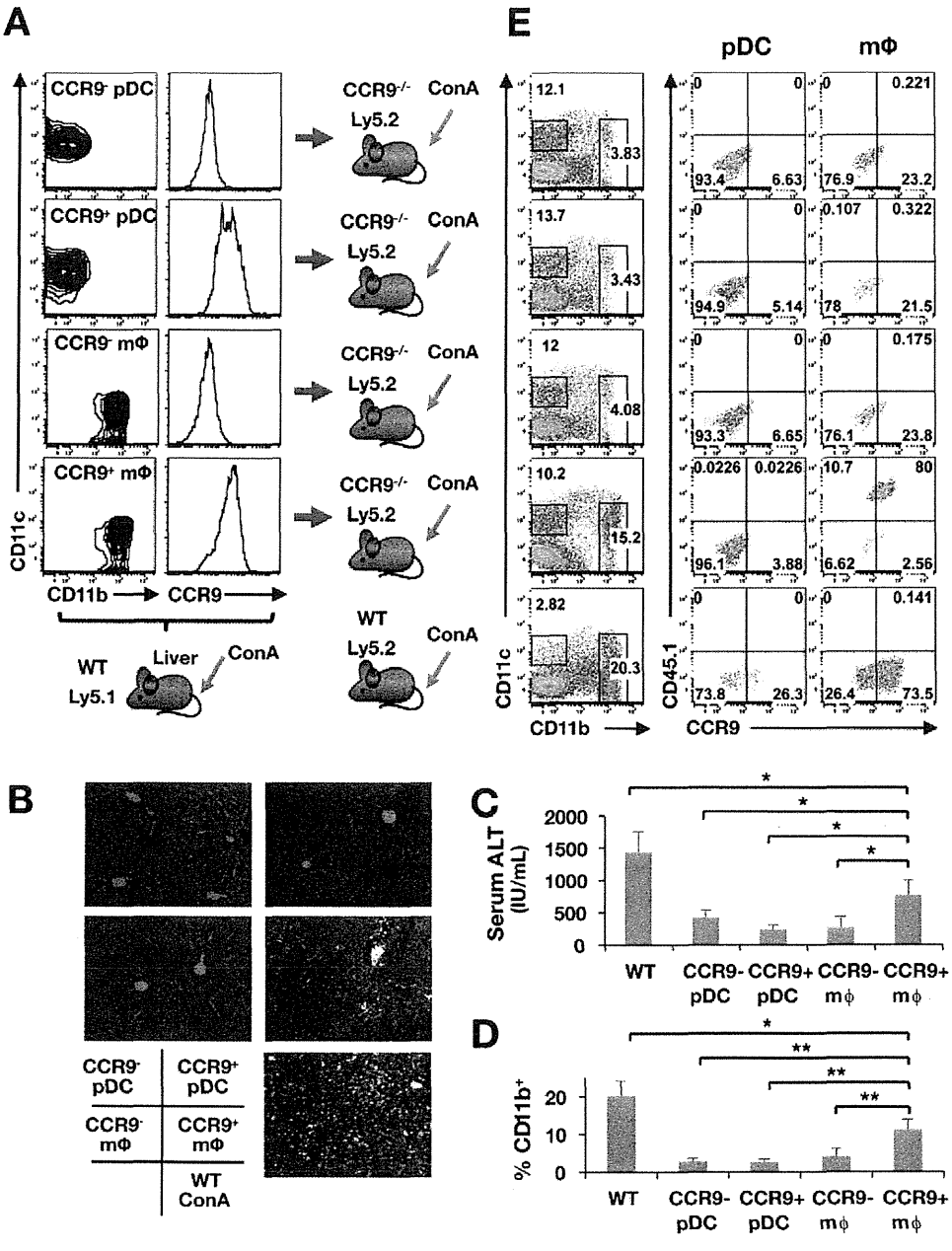

Figure 5. CCR9$^+$ macrophages are key inflammatory cells for con A–induced T-cell hepatitis. (*A*) Experimental design. CCR9$^+$ and CCR9$^-$ macrophages and CCR9$^+$ and CCR9$^-$ pDCs were isolated from the liver of con A–treated Ly5.1$^+$ mice. Mice were divided into 5 groups as follows: *CCR9*$^{-/-}$ mice transferred with CCR9$^-$ pDCs (n = 4), *CCR9*$^{-/-}$ mice transferred with CCR9$^+$ pDCs (n = 4), *CCR9*$^{-/-}$ mice transferred with CCR9$^-$ macrophages (n = 4), *CCR9*$^{-/-}$ mice transferred with CCR9$^+$ macrophages (n = 4), and WT mice (n = 4). Then, all mice were immediately injected with con A. (*B*) Representative photomicrographs of H&E-stained sections of the liver. Data are representative of each group. (*C*) Serum ALT level. Data show mean ± SEM (n = 4/group). $^*P < .05$. (*D*) Mean percentage of macrophage (CD11b$^+$) subsets in the liver from 5 groups. Data show mean ± SEM (n = 4/group). $^*P < .05$, $^{**}P < .01$. (*E*) CD11b and CD11c staining on liver mononuclear cells (*left panel*) and CCR9 and CD45.1 staining for pDC and macrophage subsets (*right panel*) in the liver from 5 groups. Data are representative of 4 independent experiments.

administration did not develop hepatitis (Supplementary Figure 7*C* and *D*).

In addition, we showed that the ratio of IFN-γ–expressing Th1 cells, but not IL-17A–expressing Th17 cells, was markedly increased in the liver of con A–treated *CCR9*$^{-/-}$ mice with the transfer of CCR9$^+$ macrophages, but not in the liver of con A–treated *CCR9*$^{-/-}$ mice without the transfer (Supplementary Figure 8).

Neutralizing Anti-CCL25 mAb Attenuated con A–Induced Liver Injury

To directly evaluate the possible contribution of CCR9/CCL25 blockade to the clinical efficacy of the treatment of acute hepatitis (AH), we examined whether neutralizing anti-CCL25 mAb was effective in preventing con A–induced hepatitis. As expected, administration of anti-CCL25 mAb significantly ameliorated con A–induced liver injury; anti-CCL25 mAb-treated mice showed less liver damage (Figure 6*A*) and lower serum levels of transaminase (Figure 6*B*) than isotype mAb-treated con A–treated mice. The number of CCR9$^+$ macrophages in the anti-CCL25 mAb-treated con A–treated group was significantly lower than in the isotype mAb-treated con A–treated group, whereas the number of CCR9$^+$ pDCs was not statistically different between the isotype mAb and anti-CCL25 mAb-treated con A–treated groups (Figure 6*C* and *D*). Interestingly, the expression of TNF-α in CCR9$^+$ macrophages in the anti-CCL25 mAb-treated con A–treated group in response to in vitro lipopolysaccharide stimulation was significantly lower than in the

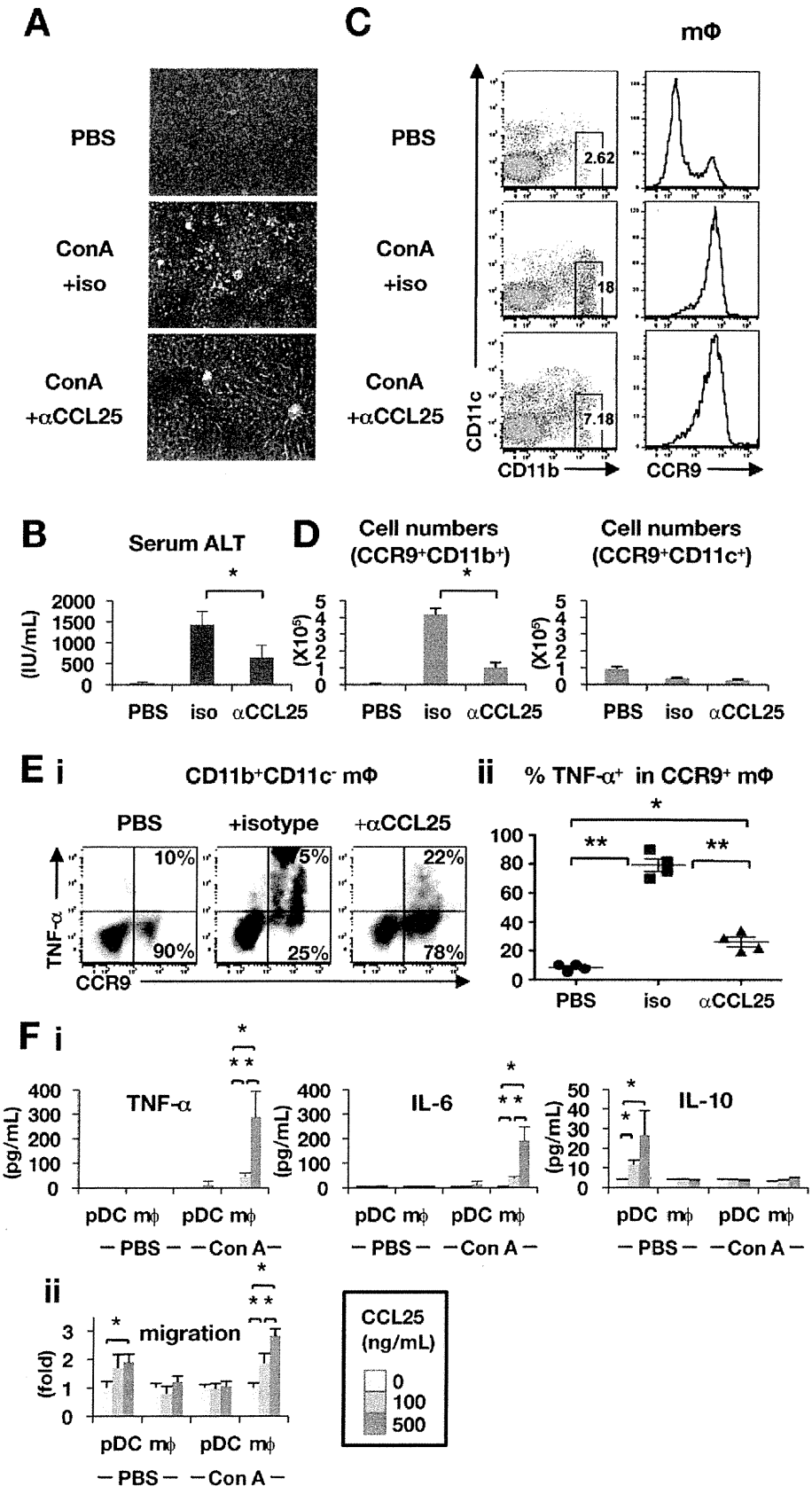

Figure 6. Neutralizing anti-CCL25 mAb treatment ameliorates con A–induced liver inflammation. (*A*) Photomicrographs of H&E-stained sections of the liver from PBS-injected, con A/isotype mAb-injected, and con A/anti-CCL25 mAb-injected mice. Data are representative of each group (n = 4). (*B*) Serum ALT level. Data show mean ± SEM (n = 4/group). $^{*}P < .05$. (*C*) CD11b and CD11c staining on liver mononuclear cells (*left panel*) and CCR9 staining for macrophage subsets (*right panel*) in the liver from 3 groups. Data are representative of 4 independent experiments (n = 4/group). (*D*) Absolute cell numbers of $CCR9^{+}CD11b^{+}$ cells (*left panel*) and $CCR9^{+}CD11c^{+}$ cells (*right panel*) in the liver from 3 groups. Data show mean ± SEM (n = 4/group). $^{*}P < .05$. (*Ei*) Intracellular TNF-α and surface CCR9 expression and (*Eii*) mean percentage of TNF-α^{+} cells in macrophages of the liver from 3 groups. Cells were stimulated with lipopolysaccharide for 6 hours, followed by surface and intracellular staining. Data show mean ± SEM (n = 4/group). $^{*}P < .05$, $^{**}P < .01$. (*Fi*) Production of TNF-α, IL-6, and IL-10, in response to CCL25. $CD11b^{+}CD11c^{-}$ macrophages or $CD11b^{-}CD11c^{low}$ pDCs obtained from the liver of PBS- or con A–treated mice were cultured with CCL25 (0, 100, 500 ng/mL). (*Fii*) Migration assay. Fold increase of migration by CCL25 compared with the baseline (without CCL25 incubation) was calculated. Data show mean ± SEM (n = 4/group). $^{*}P < .05$, $^{**}P < .01$.

isotype mAb-treated con A-treated group (Figure 6*E*); this suggests that up-regulated CCL25 under inflammation contributes to both the migration and activation of CCR9$^+$ macrophages.

Notably, macrophages obtained from the liver of con A-treated mice—but not macrophages and pDCs from the liver of PBS-injected mice and pDCs from the liver of con A-treated mice—produced a significantly higher amount of TNF-α and IL-6 in response to CCL25 in a dose-dependent manner (Figure 6*Fi*). By contrast, pDCs from the liver of PBS-injected mice, but not macrophages and pDCs from the liver of con A-treated mice, produced significantly higher amounts of IL-10 in response to CCL25 in a dose-dependent manner (Figure 6*Fi*). We further performed an in vitro migration and cell activation experiment using macrophages and pDCs obtained from the liver of PBS- and con A-treated mice. As expected, the migratory ability of pDCs from the liver of PBS-injected mice and macrophages from the liver of con A-treated mice, both of which express CCR9, was significantly increased in the presence of CCL25 (Figure 6*Fii*).

TNF-α–Expressing CD14$^+$CD16^{high}CCR9$^+$ Monocytes Were Markedly Increased in the Peripheral Blood of Patients With AH

Finally, we attempted to apply the present results in mice to human AH, such as viral hepatitis and autoimmune hepatitis. To this end, we assessed the phenotypes of the peripheral blood (PB) in patients with AH, patients with chronic hepatitis (CH), and normal controls (NCs). The precise characteristics of each group are summarized in Supplementary Table 1. In particular, we focused on CD14$^+$CD16$^+$ cells in PB samples, because it has been reported that the subpopulation of CD14$^+$CD16$^+$ monocytes produces a large amount of TNF-α and other proinflammatory cytokines to participate in inflammation.[28] First, the proportion of CD14$^+$CD16^{high} monocytes, but not CD14$^+$CD16^{low} or CD14$^-$CD16^{high} monocytes, was significantly increased in the PB of patients with AH as compared with that of NCs and patients with CH (Figure 7*A*, *left*, and *B*). Furthermore, the positive percentage of CCR9$^+$ cells in CD14$^+$CD16^{high} monocytes was significantly higher in the PB of patients with AH than in that of NCs or patients with CH (Figure 7*A*, *right*, *C*, and *D*). Importantly, TNF-α was preferentially expressed on CD16^{high}CCR9$^+$ but not on CD16^{high}CCR9$^-$ subpopulations in the PB of patients with AH (Figure 7*E*).

Discussion

We here identify CCR9$^+$ macrophages as key inflammatory cells of con A-induced AH in mice. Figure 7*F* gives a schematic view of the current study. Our results clearly show that CCR9$^+$ macrophages played a key role in promoting proliferation of CD4$^+$ T cells and generation of IFN-γ-producing Th1 cells as well as NKT cell activation in con A-induced T-cell hepatitis.

To investigate the mechanism of the breakdown of liver tolerance in the inflammatory state, we initially focused

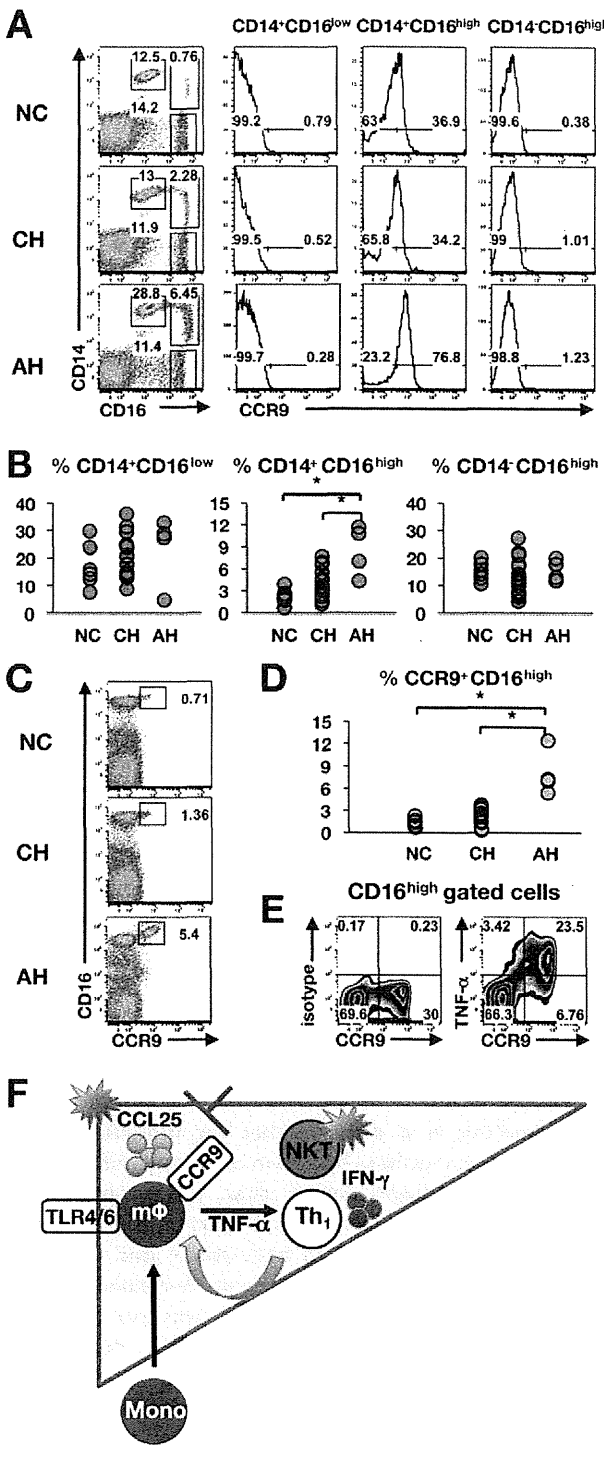

Figure 7. TNF-α–expressing CD14$^+$CD16^{high}CCR9$^+$ monocytes emerge in the PB of patients with AH. (*A*) CD14 and CD16 staining (*left panel*) and CCR9 staining on indicated subsets of cells (*right panel*) isolated from the PB of NCs, patients with CH, and patients with AH. (*B*) Mean percentage of CD14$^+$CD16^{low}, CD14$^+$CD16^{high}, and CD14$^-$CD16^{high} monocytes. $^*P < .05$. (*C*) CCR9 and CD16 staining on the PB isolated from 3 groups. (*D*) Mean percentage of CCR9$^+$CD16^{high} populations. $^*P < .05$. (*E*) Intracellular TNF-α and surface CCR9 staining on CD16^{high} gated cells of PB from AH. (*F*) Suggested immunologic mechanism through con A–induced acute liver inflammation. After administration of con A, CCR9$^+$ macrophages migrated to the CCL25 up-regulated liver promote proliferation of CD4$^+$ T cells and generation of IFN-γ–producing Th1 cells as well as NKT cell activation. mφ, macrophages; mono, monocytes.